Thesis submitted in partial fulfillment of the requirement for the degree of Master of Chemical Engineering

SIMULTANEOUS REMOVAL OF OFLOXACIN & RHODAMINE B DYE FROM WASTEWATER BY ACTIVATED JAMUN SEED POWDER

A small attempt toward the partial accomplishment in the Department of Chemical Engineering

By

ANWESHA SINHA

Class Roll No: 002210302028

Exam Roll No: M4CHE24028

Registration no 163451 of 2022-2023

Under the guidance of

(Prof.) Dr.Saswata Bose

&

(Prof.) Dr. Mehabub Rahaman

DEPARTMENT OF CHEMICAL ENGINEERING

JADAVPUR UNIVERSITY

Kolkata – 700032

SELF DECLARATION OF CREATIVITY OF ACADEMIC PRINCIPLES

I hereby confirmed that the thesis work contains on the basis of a literature survey and original research work by the undersigned candidate, as part of "The **Master of Engineering in Chemical Engineering** studies. All information in this document has been obtained and presented in accordance with academic rules and ethical conduct

ANWESHA SINHA

Class Roll No: 002210302028

Exam Roll No: M4CHE24028

Registration no 163451 of 2022-2023

Project Title: SIMULTANEOUS REMOVAL OF OFLOXACIN & RHODAMINE B DYE FROM WASTEWATER BY ACTIVATED JAMUN SEED POWDER

Signature:

Date:

CERTIFICATION

This is to certify that Ms Anwesha Sinha, a final year student in the Master of Chemical Engineering examination in the Department of Chemical Engineering, Jadavpur University, bearing Registration No: 163451 of 2022-2023 has successfully completed the thesis work entitled **"SIMULTANEOUS REMOVAL OF OFLOXACIN & RHODAMINE B DYE FROM WASTEWATER BY ACTIVATED JAMUN SEED POWDER"** under the guidance of **Prof. (Dr.) Saswata Bose sir** and **(Prof.)Dr. Mehabub Rahaman** during master degree curriculum. This work has not been reported earlier anywhere and can be approved for submission in partial fulfilment of the requirements for the Master of Engineering in Chemical Engineering.

23/8/24

(Prof.) Dr. Saswata Bose

Supervisor

Department of Chemical Engineering

Jadavpur University

Assistant Professor
CHEMICAL ENGINEERING DEPARTMENT
JADAVPUR UNIVERSITY
Kolkata-700 032

Mehabub Rahaman 23/8/24

(Prof.) Dr. Mehabub Rahaman

Co-supervisor

Department of Chemical Engineering

Jadavpur University

Associate Professor
CHEMICAL ENGINEERING DEPARTMENT
JADAVPUR UNIVERSITY
Kolkata-700 032

P Das 23/8/24

(Prof.) Papita Das

Head of the Department

Department of Chemical Engineering

Jadavpur University

HEAD
CHEMICAL ENGINEERING DEPARTMENT
JADAVPUR UNIVERSITY
Kolkata-700 032

Dipak Laha 23.08.24

Dean

Faculty of Engineering & Technology

Jadavpur University

DEAN
Faculty of Engineering & Technology
JADAVPUR UNIVERSITY
KOLKATA-700 032

CERTIFICATE OF APPROVAL

As a creditable study of an engineering subject completed and presented in a way that is acceptable to support its acceptance as a requirement for the degree for which it has been submitted, this thesis is officially accepted. This approval signifies that the undersigned accepts the thesis only for the purpose for which it is presented and does not endorse any statements made, opinions expressed, or conclusions reached within.

(Prof.) Dr. Saswata Bose	**(Prof.) Dr. Mehabub Rahaman**	**Signature of the Examiners**
Supervisor	**Co-supervisor**	
Department of Chemical Engineering	**Department of Chemical Engineering**	
Jadavpur University	**Jadavpur University**	

ACKNOWLEDGEMENT

At first, I would like to thank my respected guides, **(Prof.) Dr. Saswata Bose Sir & (Prof.) Dr. Mehabub Rahaman Sir.** Without their active guidance, valuable technical support, valuable advice, help, and supervision, I would not have been able to complete my project. I am very grateful to my guide for providing me with the golden opportunity to accomplish this project.

I must thank everyone in the Chemical Engineering department for helping me with my project work.

I am very grateful to all laboratory technicians in the chemical engineering department; their sincere help has helped me make my work easier to carry forward.

I am very grateful to the head of the department, Prof. Papita Das, and all the respected professors of the Chemical Engineering department.

Finally, I am very grateful to my guide as well as my supervisors, Prof. (Dr.) Saswata Bose sir and Prof. (Dr.) Mehabub Rahaman sir, for their continuous support, advice, and help during the thesis work.

A special thanks to my parents and my friends.

Thanking You,

ANWESHA SINHA

Class Roll No: 002210302028

Registration no 163451 of 2022-2023

Department of Chemical Engineering

ABSTRACT

Through the processes of carbonization and chemical activation, a low-cost adsorbent was created in this work using bio waste jamun seed (Syzygium cumini) that was previously available. It was used to extract Rhodamine B, a color dye, and the prescription medication ofloxacin from their aqueous solutions. Using "Field Emission Scanning Electron Microscope" (FESEM), "Fourier Transform Infrared Spectroscopy" (FTIR), and particle size analysis, the surface morphology and surface area of the repaired activated Jamun seed dust were examined. It was discovered that the surface area of activated jamun seed (ACJS) was 366.39m^2/g. Following CHNS analysis, the powdered jamun seed had a carbon content of 55.68%.

After three hours, 90-99 % of the ofloxacin in the aqueous solution was eliminated while maintaining the mixture's pH at 5. Additionally, activated jamun seed powder (ACJS) removed 50% of the Rhodamine B from the aqueous solution in 3 hours while keeping the pH of the solution at 5. This was accomplished with activated jamun seed powder (ACJS).

ACJS's maximum adsorption capacity was 39.97 mg/g. With R^2 = 0.99158 and 0.99732, the adsorption kinetics were in accordance with a linear pseudo 2^{nd} order model. The Langmuir linear isotherm fitted with experimental data was demonstrated by the isotherm investigation. Thermodynamics research shows that adsorption is a viable, exothermic process. The powdered jamun seed is the source of activated carbon, which is also inexpensive and may be used for up to many cycles without lowering the effectiveness of OFC and Rhodamine B removal.

Nomenclature

Symbols	Description
C_i	Initial concentration
C_o	Final Concentration after removal
Re	Removal efficiency
T	Temperature
Q_t	Adsorption Capacity at time t

Abbreviations

Initialism	Description
AC	Activated carbon
OFC	Ofloxacin
Rhb	Rhodamine B
JS	Jamun Seed
ACJS	Activated Jamun seed
PJS	Pyrolyzed Jamun seed
API	Active pharmaceutical ingredient
SEM	Scanning Electron Microscope
CHNS	Carbon Hydrogen Nitrogen Sulphur analysis
FTIR	Fourier Transform Infrared Spectroscopy

List of Tables

Page No.

Table.1 Ofloxacin and its properties…….7

Table.2 Rh B and its properties…..……..……...9-10

Table.3 CHNS data of PJS and JS…….....31

Table.4 Experimental results on various adsorption isotherm……...40-41

Table.5 Results on adsorption kinetic model……..……...45-46

Table.6 Thermodynamics studies of (a) OFC & (b) Rhodamine B……..…..…51-52

List of Figures

Page No.

Figure.1 Structure of Ofloxacin…….....7

Figure.2 Structure of Rhodamine B……...9

Figure.3 Experimental steps to prepare ACJS from jamun seed (JS)……....….18

Figure.4 Various ratio KOH activated Jamun seed powder…….18

Figure.5 Standard plot to determine the concentration in aqueous solution of OFC & Rh B ….....22

Figure.6 SEM morphology of (a) JS and (b) ACJS……..……..32

Figure.7 EDS spectrum of ACJS……..33

Figure.8 FTIR spectrum of (a) JS and (b) ACJS……..34

Figure.9 Effect of pH of solution…….36

Figure.10 Effect of initial concentration of OFC on removal efficiency of ACJS……37

Figure.11 Effect of ACJS dosage on removal of OFC……...38

Figure.12 Effect of temperature on the removal of OFC……...39

Figure.13 (a). Langmuir linear adsorption isotherm plot……...42

(b). Langmuir Nonlinear adsorption Isotherm plot……..……..42

Figure.14 (a). Linear Freundlich adsorption isotherm model……....43
(b). Non linear Freundlich adsorption isotherm model……...…..44
Figure.15 Temkin adsorption isotherm……..45
Figure.16 (a).Linear pseudo 1^{st}oreder kinetics……...47
(b). Linear pseudo 2^{nd} oreder kinetics……48
Figure.17 The plot of q_t vs $t^{(1/2)}$ for Intra particle diffusion model……49
Figure.18 Thermodynamic study on adsorption ……50
Figure.19 Determination of activation energy on adsorption……51

INDEX

CONTENT	PAGE NO.
SELF DECLARATION OF CREATIVITYOF ACADEMIC PRINCIPLES	**(i)**
CERTIFICATION	**(ii)**
CERTIFICATE OF APPROVAL	**(iii)**
ACKNOWLEDGEMENT	**(iv)**
ABSTRACT	**(v)**
LIST OF NOMENCLATURE & ABBREVIATIONS	**(vi)**
LIST OF TABLES	**(vii)**
LIST OF FIGURES	**(vii-viii)**
CHAPTER 1	
INTRODUCTION	4
1. Introduction	5
1.1 Ofloxacin and its properties	6-7
1.2 Rhodamine B Dye and its properties	8-9
1.3 Purification technologies of removal of OFC and RhB from wastewater	10-12
1.4 Activated carbon as the adsorbent	12-13
1.5 Objective of the work	14-15
CHAPTER 2	
EXPERIMENTAL AND METHODOLOGY	17
2.1. Chemicals and biomass	17
2.2. Preparation of activated carbon	17-19
2.3. Characterization	19
2.4.1. Ultimate analysis of JS	19
2.4.2. Proximate analysis of JS	19-20
2.5.1 .Scanning electron microscope (SEM) and EDS analysis	21
2.5.2. Fourier transform infrared (FTIR) spectroscopy	21

2.6. Batch adsorption studies 21-23
2.7. Isotherm models to represent the adsorption process 23
2.7.1. Langmuir isotherm model 23-24
2.7.2. Freundlich isotherm model 24-25
2.7.3. Temkin isotherm model 25
2.8. Adsorption kinetic studies 25-26
2.8.1. Pseudo first order kinetics 26
2.8.2. Pseudo second order kinetics 27
2.9. Intra - particle diffusion model 27-28
2.10. Adsorption thermodynamic studies 28-29

CHAPTER 3

RESULTS AND DISCUSSION

3.1. Characterization 31
3.1.1. Proximate and elemental analysis 31
3.1.2. SEM (FESEM) - EDS 31-33
3.1.3. FTIR analysis 33-34
3.2. Batch adsorption studies 35
3.2.1. Effect of solution pH 35-36
3.2.2. Effect of initial concentration OFC and RhB 36-37
3.2.3. Effect of adsorbent dosage 37-38
3.2.4. Effect of temperature 38-39
3.3. Isotherm studies 39-45
3.4. Kinetic Studies on Adsorption 45-49
3.5. Thermodynamics study on adsorption of OFC & RhB 49-52

CHAPTER 4

4. Conclusion 55

5. References 56-63

CHAPTER 1

INTRODUCTION

1. Introduction

Pharmaceutical medications, which come from human urine, expired medication, hospitals, industrial effluent, etc., are currently one of the most developing pollutants for the environmental eco-system. Because of the overuse of medications for a variety of objectives, including veterinary care, fish farming, agriculture, and human lives, there is an increased accumulation of pharmaceuticals in wastewater [1]. Various classifications of pharmaceutical residue, including antibiotics, steroids, non-steroids, narcotic analgesics, inhalants, etc., are found in relation to the usage of human livestock in the environment. Some of these are very soluble in water, poorly biodegradable, and filtered naturally into groundwater, which affects the aquatic ecosystem as well as other areas of the environment by causing various health problems.

Antibiotics are among these medications that are most frequently used in human animals, and they are also the primary source of pharmaceutical pollutants found in hotel trash, expired medications, and pharmaceutical effluents [2, 3]. Active pharmaceutical ingredients (API) of antibiotics are released in significant quantities by pharmaceutical wastewater. Of the antibiotic APIs, a small number dissolve easily in water, while the remainder is either insoluble or only partially soluble. Antibiotics can have detrimental effects on algae and can make bacterial infections more resistant [4, 5]. It is occasionally the case that antibiotics increase bacterial health resistance while simultaneously improving physiological alterations and health proficiency [6, 7]. Additionally, antibiotics aid in compensating for microbial mutations and restoring physical fitness [8].

It is regrettable to report that because antibiotic residue is not biodegradable, it can create major health problems when it is disposed of carelessly and ends up in the environment, including the surface and ocean. Certain non-biodegradable additives may exhibit stability in the removal stage of the traditional activated sludge process used in sewage treatment [9, 10]. These pollutants then spread throughout the environment through a number of mechanisms.

1.1. Ofloxacin and its properties :

Ofloxacin (OFC) is one of the most commonly used antibiotics among them. It belongs to the class of antibiotics known as fluorinated quinolones [11]. An antibiotic of the second generation is ofloxacin [12]. 50% of the enantiomer of dextro - Ofloxacin and 50% of lev-Ofloxacin make up a raceme combination of OFC. When it comes to antibacterial activity against gram (+) and gram (-) bacteria, the (-) isomer has roughly 10-100 times more influence than the (+) isomer [13]. Since ofloxacin cannot be completely digested by the physical body, it is primarily excreted in urine, which is then deposited into city or hospital drainage systems. The ecosystem's level of chlorophyll was reduced by OFC, which may have reduced the microscopic population's ability to perform photosynthetic activities [14, 15].

Furthermore, OFC was not completely eliminated by the wastewater treatment plant. The remaining OFC in wastewater-treated plant sewage can have an impact on water from the surface, the soil, and the slit [16]. Antimicrobial medication addiction may be detrimental to the natural balance of bacteria and aquatic habitats. Because they resemble microorganisms in structure, cyano bacteria are the aquatic species most susceptible to fluoroquinolones. The bacterial community's morphology changed and its degree of difficulty significantly dropped after being exposed to OFC. This implies that OFC might affect the capacity of prokaryotic communities to survive and might throw off the ecosystem's delicate equilibrium.

OFC is used for a variety of conditions, including urinary tract infections, nose infections, pneumonia, diarrhea, and lower respiratory issues. It is also used as eye and ear drops (Oflox, Oflatop) and as a tablet (Zancin 200, "O2"). In human urine, 80% of the OFC is discharged and stays constant [17].

Although OFC has very little biodegradation, biodegradability is a key component in the breakdown of antibiotic medications in STP [18]. Severe health issues such as fever, skin rash, constipation, nervousness, anxiety, and abdominal or chest pain may arise from consuming more ofloxacin than the body can tolerate. An overwhelming amount of OFC can result in severe anxiety, agitation, and other lasting nerve damage. Therefore, it's critical to remove OFC from

effluent. Below are some examples of OFC's physical characteristics and environmental effects [19].

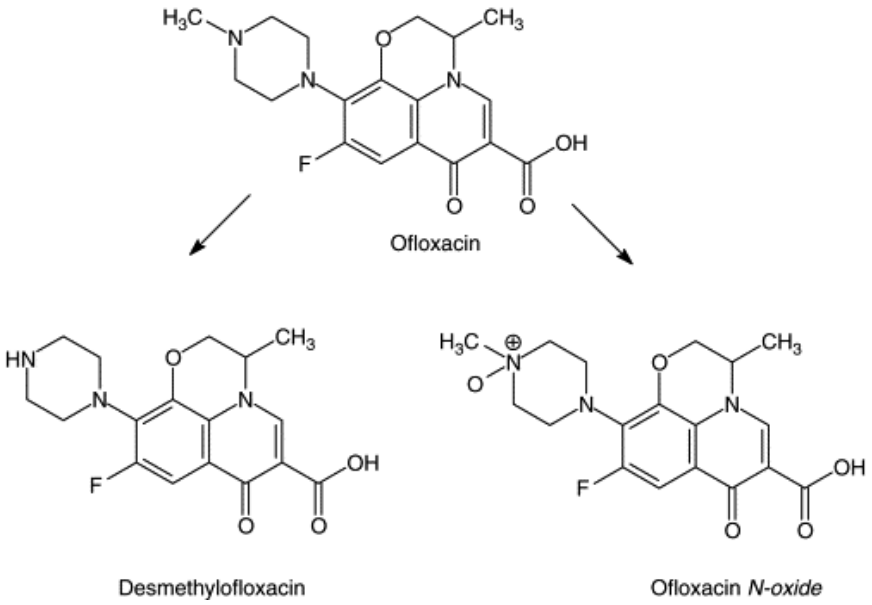


Figure 1 Structure of Ofloxacin

Table 1: Properties of Ofloxacin

IUPAC name	((RS)-7-9-fluoro2,3-dihydro-3-methyl-10-(4-methyl-1-piperazinyl)-7-oxo-7H-pyrido[1,2,3-de]-1,4-benzoxazine-6-carboxylic acid)
Molecular weight	361.388
Molecular formula	$C_{18}H_{20}FN_3O_4$
Melting point	254^{o}C
Solubility	Soluble in aqueous solution between pH 2 to pH 5. Sparingly soluble in aqueous solution with pH 7.

1.2. Rhodamine B Dye and its properties:

The expansion of industries and agriculture has led to an increase in environmental pollution, which is a serious problem in modern times. Many pollutants, especially dyes, are being released by these sectors. Numerous industries, including the textile, culinary, cosmetics, paint, pharmaceutical, printing, leather, and plastic sectors, depend heavily on dyes for their operations. In aquatic ecosystems, dyes can have detrimental effects even in tiny concentrations, have the potential to obstruct light from entering water systems, which can disturb aquatic species' biological processes and result in major health issues, illnesses, allergies, dermatitis, skin irritation, respiratory toxicity, and even cancer.

Based on their nuclear structures, dyes can be classified as anionic, nonionic, or cationic. Among these is Rhodamine B, a basic red cationic dye that dissolves in water and is frequently employed as a water tracer because of its superior photophysical characteristics. One of the earliest synthetic dyes, Rhodamine B, is a member of the xanthene class.

Because of their high degree of micro porosity, huge surface area, and good performance, activated carbons are effective adsorbents in biomass adsorbents. However, the precursor, activators, and production methods employed all have a significant impact on the effectiveness of activated carbons. One major obstacle to the commercial manufacture of activated carbon is the utilization of costly, nonrenewable precursors, such as conventional long-term heating methods.

The use of biological materials, such as biomass and agricultural waste, is a highly effective choice for adsorption because of their quantity and renewability, which investigated alternate sources for adsorption. The first step in the creation of activated carbon is carbonization, regardless of the use of activation treatment. In this procedure, organic materials can be converted into elemental carbons using traditional or microwave-assisted pyrolysis. It is the most extensively used approach and is also inexpensive.

Microwave-assisted pyrolysis is now a popular technique due to its quick and selective heating mechanism, which surpasses the limitations encountered in conventional heating methods. The media molecules in this process undergo high-frequency vibrations and frictional collisions,

leading to a sharp rise in temperature. This results in a shorter treatment time, owing to the utilization of microwave energy.

It has been demonstrated that the use of activated carbons based on biochar has a high level of efficiency in sorption applications. To increase the functionality, selectivity, specific surface area, and adsorptive qualities of various adsorbates, acid activation is a widely used, simple procedure that can usually be completed in a single step. Multi-stage acid activation is not well studied. Through 1-step and 2- step KOH activation, the potential of activated carbons made from empty fruit bunches used in palm oil was to be assessed in this study. An analysis was done on the impacts of response factors such as contact time, metal ion concentration, and solution pH. Two-parameter adsorption isotherms were utilized to assess the activated carbon's adsorption capacity for Rhodamine B (Rh B).

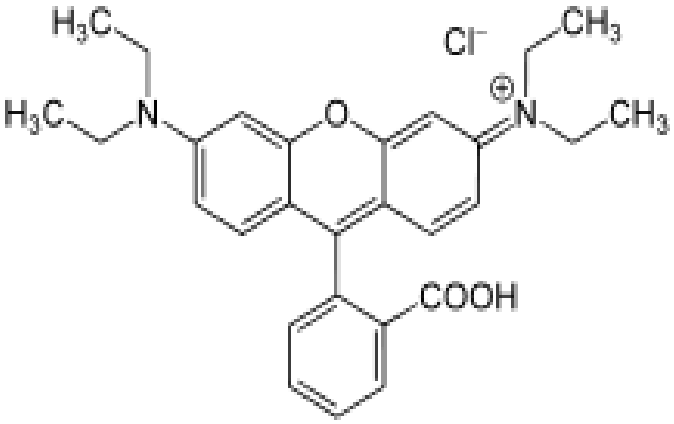


Figure 2 Structure of Rhodamine B

Table 2: Properties of Rhodamine B

IUPAC name	9-(2-Carboxyphenyl)-6-(diethylamino)-*N*,*N*-diethyl-3*H*-xanthen-3-iminium chloride

Molecular weight	497.02
Molecular formula	$C_{28}H_{31}ClN_2O_3$
Melting point	210 to 211 °C (410 to 412 °F; 483 to 484 K) (Decomposes)
Solubility	The solubility of Rhodamine B in water varies by manufacturer, and has been reported as 8 g/L and ~15 g/L, while solubility in alcohol (presumably ethanol) has been reported as 15 g/L. Chlorinated tap water decomposes Rhodamine B.

1.3 Purification technologies of removal of OFC and RhB from wastewater

- **Physical process:** Screening, sedimentation, flotation, and granular media filtration are all done in this unit. The entire procedure does not undergo nanoscale purification. This method only removes pollutants from wastewater up to a particular point of purification. However, this water is unfit for human consumption due to the small levels of impurities present.

- **Biological process:** Biological unit procedures include the trickling filter, the aerated lagoon, and the activated sludge process.

- **Activated sludge process:** Large amounts of foam are created during this process, along with hazardous gases like methane and sludge that contains a variety of dangerous bacteria, viruses, and other microorganisms. The main drawback of this approach is operating costs.

- **Chemical processes:** The following categories—discussed below—can be used to group the chemical processes:.

- **Photocatalytic Degradation:** In this procedure, solar sensitivity is used in low light. Plus, the process is incredibly expensive. The main drawback of this procedure is that it

is quite expensive to run, and the tools utilized in this experiment are also highly expensive. For surface treatment, photocatalytic oxidation is not employed. In addition, the technique is intricate.

- **Membrane separation:** The method works well for home use, but it was never applied on an industrial scale because of maintenance costs, the use of certain dangerous chemicals and solvents, and the permanent destruction of the membrane. Larger species obstruct the pore and reduce the membrane's porosity, resulting in an extremely slow rate of filtration.

- **Coagulation:** While the investment in this procedure is cheaper, the cost of operation and maintenance is much higher. Occasionally, a significant amount of residual, non-biodegradable sludge formed during this procedure has a negative effect on the environment.

- **Adsorption:** These days, both industrial and home applications heavily rely on the adsorption process. There are two stages to this method: a solid phase and a liquid or gaseous phase. Adsorbent (solid phase) is one, and adsorbate is another. Adsorption can be divided into two categories: chemical adsorption and physical adsorption. The former is brought about via hydrogen bonding, ion exchange, Van der Waals forces of attraction, and particle size.[39, 40] The technique is widely utilized because it is easy to use, inexpensive, and cost-effective. Adsorbents are extremely porous materials with a lot of surface area on the outside. Diffusing molecules are drawn to the neighboring surface by magnetic forces, where they remain for a maximum amount of time.

  The temperature of the solution plays a crucial role in the adsorption process in batch research; the highest adsorption occurred primarily at ambient temperatures (25–30°C).

- Pollutant solubility determines how pollutants adsorb through several mechanisms. In comparison to insoluble contaminants, chemicals that are soluble in water adsorb more.

Below are the qualities of an ideal adsorbent:

- A large surface area is required.
  Pore distribution is uniform, and the prepared adsorbent should have a high removal capability of the pollutant.
- The ability to reuse and recycle is also crucial components.
  This is an exothermic process that depends on temperature and is a surface phenomenon.

1.4. Activated carbon as the adsorbent

The two primary forms of activated carbon (AC) are granular and powdered forms. Chemical activation or gas enactment of carbon follows the intentional synthesis of one or both of these AC. Activated carbon is a micro-crystalline form of carbon that can be produced from aceous materials such as coal, wood, tires, lignite, organic waste solids, luffa sponge, and willow peat. In order to reduce the cost of the adsorption framework, AC has lately been recovered from agricultural wastes such as bagasse, sugar cane, rice husks, mango peels, coconut shells, various tree leaves and barks, fruit seeds, etc.

An atmosphere of nitrogen is used during the preparation of activated carbon in order to eliminate air, avoid yield loss, and prevent the production of early oxygen. When pyrolyzing in a furnace, the temperature range rises from 450 to 700 °C. A lot of activated carbon is used to remove natural micro pollutants from wastewater because of its high porosity, greater surface area, and dormant nature, security throughout a wide pH range, appropriate pore size, and existence of useful, diverse organic functional groups. Granular activated carbon (GAC) and powder activated carbon (PAC) are two distinct adsorbent materials that differ primarily in that GAC contains larger particles and a reduced outer surface area.

The surface area plays a major role in the adsorption process. The interior surface defines the maximum potential adsorption process capacity, whereas the outside surface area influences the rate of mass exchange during adsorption. The material's inward surface area also influences the

adsorption of normal particles onto the interior surface. Thus, the pores shouldn't be excessively small in order to promote the adsorption of important particles. Although there are many adsorbents on the market, activated carbon is the most widely used and practical. Although there are many adsorbents on the market, activated carbon is the most widely used and practical. It eliminates organic pollutants to a large extent from both the liquid (water) and gaseous phases.

Additionally, it extracts low-water-soluble molecules from water by adsorbing them. This is used to eliminate color from the solution as well as non-biodegradable organic micro pollutants and pharmaceutical residue. Activated carbon is made using a natural resource, such as fruit shells, bark, hardwood, tree leaves, etc., and the process is rather straightforward.

When compared to other tree species, the extract from jamun seeds offers several advantages, including a greater volume and superior binding affinity, a broad surface area, and fewer nutrient requirements. Jamun seeds (Syzygium cumini) are an inexpensive source of feedstock for bio-adsorption since they are easy to grow in large quantities in the environment. Due to its availability, affordability, and excellent physiochemical properties, jamun seed has been utilized as one of the sources of activated carbon in recent times [32, 36]. Activated carbon was successfully made from jamun seeds in this experiment by first pyrolyzing them in a muffle furnace and then chemically activating them using potassium hydroxide. It was chosen to use jamun seed as the primary raw material for activated carbon since it is a common municipal waste and is readily available. Because impregnated activated carbon removes the most ofloxacin and Rhodamine B from wastewater, potassium hydroxide is utilized as a precursor. Adsorbent dosages, contact time, and beginning concentration were among the process variable elements that were adjusted in order to find the best conditions for carrying out the adsorption experiment. Research on kinetics is conducted in addition to parameter research. Finding out if the produced adsorbent could be reused was the aim of the regeneration study.

1.5 Objective of the work

Following the review of the previously stated literature, the specialist found a number of methods for purifying water, such as advanced oxidation, membrane filtration, electro coagulation, sonochemical degradation, fenton degradation, and many more. While these

methods offer advantages for treating water, they also have a number of disadvantages. Sonochemical degradation and membrane filtering have the primary drawback of being quite expensive due to their advanced oxidation processes. The Pyrex glass must be handled with extreme caution during the photocatalytic degradation process, and the equipment is expensive and has a complicated mechanism. Adsorption, on the other hand, is a very practical method of removing contaminants from wastewater. The process of adsorption is simple and affordable.

Analogously, a variety of adsorbents are available for industrial use, including silica gel, zeolite, neutral alumina, and polymeric adsorbents. In contrast, AC is less expensive than several adsorbents, and its raw materials come from natural biomass sources, making it the ideal alternative for wastewater treatment, according to the literature review mentioned above. Hospital wastewater, river wastewater, seawater, etc. all contain pharmaceuticals such as ofloxacin and the color Rhodamine B. Anxiety, fever, skin rash, nervousness, and abdominal and chest pain are only a few of the conditions that might arise from an improper ofloxacin and Rhodamine B intake. Therefore, it is very important to remove ofloxacin and Rhodamine B from effluent.

With activated carbon made from jamun seeds, the thesis work primarily focused on eliminating OFC and RhB from water and found that it was effective in doing so. Its solution's ability to remove OFC is improved by the activated jamun seed's sufficient potential. The following are the primary objectives of the research project:.

- Utilizing biological resources, such as leftover jamun seed, to create an adsorbent.
- A muffle furnace is used to carbonize jamun seeds at a specific temperature and then KOH is added to the carbonized seeds in varying ratios to create activated carbon.
- Batch studies were conducted to determine the effects of pH, initial concentration, and amount of adsorbent dosage, temperature, and mixing time on the adsorption process.
- The FTIR, SEM, particle size analyzer, CHNS, and proximate analyzer were used to characterize the chemically activated jamun seed.
- Evaluating different isotherms to find the amount of activated carbon produced from jamun seeds, such as the Temkin, Freundlich, and Langmuir adsorption isotherms.
- The adsorption kinetics of activated carbon derived from jamun seeds is examined.

- A thermodynamic study of the adsorption process onto the surface of activated carbon produced by jamun seeds.

CHAPTER 2

EXPERIMENTAL METHODOLOGY

2.1 Chemicals and biomass

Jamun (Syzygium cumini) fruit collected from the plantation nearby area and also procured from vegetable market. Ofloxacin was purchased from Sigma-Aldrich. Rhodamine B dye (CI 45170) was purchased from HIMEDIA (India). Potassium Hydroxide (KOH) was procured from Oasis Fine Chem., India. 25 % Ammonium Hydroxide (NH_4OH) and 37% Hydrochloric Acid (HCL) procured from Merck Specialties Pvt Ltd. Double distilled water was used throughout the experiment purposes preparing the aqueous solutions.

2.2 Preparation of activated carbon

The jamun fruit's peel and outer layer were cut off, and the seeds were gathered and continuously cleaned with water to get rid of pollutants and impurities. After seven to ten days in the sun, the seeds were dried in a hot air oven [Make: Spac-N-Service]. Hot-Air Oven (Maximum temperature: 300°C; 1.5 kW)] for 48 hours at 100°C. Following these steps, the seeds were crushed, ground, and sieved through a 250 micron mesh screen using a mortar and pestle to create a fine powder. After that, the powder is labeled as jamun seed powder (JS) in order to be used in the activation of carbon. After that, JS was chemically activated using the next two steps. The JS was carbonized in the first stage using a programmed muffle furnace (Model: Space-N-Service Muffle Furnace; Maximum temperature: 1000°C; Maximum power: 4 kW). The carbonization method involved increasing the temperature by 10°C/min from room temperature (~25°C) to 350 °C, holding that temperature for 30 minutes to eliminate organic matter, and then increasing the temperature to 650 °C at a rate of 10 °C/ min. Then, the process was maintained at 650°C for 2 hours for completion of carbonization process and lastly, it was permitted to cool down till room temperature was attained. The carbonized product was dried in an oven at 120 °C for 24 hours after being repeatedly cleaned and decanted with distilled water to remove ash. Carbonized jamun seed (CJS) was the label applied to the sample. KOH was used to chemically activate the CJS in the second phase. It was treated with a KOH aqueous solution in various weight ratios of KOH to CJS, such as 1:1, 2:1, 1:2, 1:5, and 5:1, and it was stirred magnetically for 12 hours at room temperature. Once the water's pH became neutral, the solution was filtered and rinsed with water. Following a 24-hour drying process at 120°C in a hot air oven, the chemically treated samples were crushed and put into storage containers. ACJS was the final product's name.

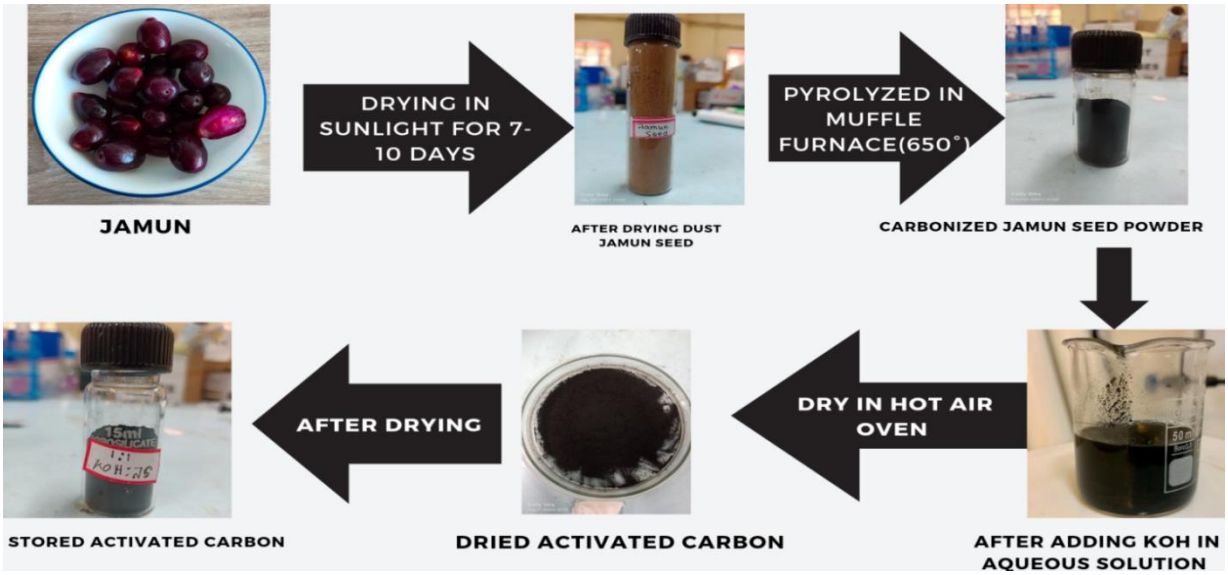


Figure: 3 Experimental steps to prepare ACJS from jamun seed (JS)

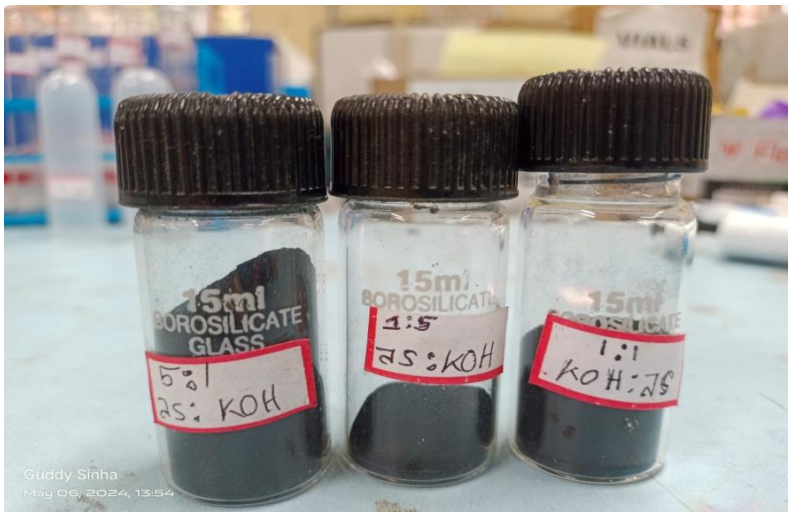


Figure: 4 various ratios KOH Activated jamun seed powder

2.3. Characterization

Using a variety of analytical techniques, the jamun seed powder (JS) and its chemically activated jamun seed powder (ACJS) were prepared. This allowed for the knowledge of the surface morphology, functional groups, surface area and porosity measurement, chemical composition, and elemental composition of the ACJS. The sections that follow provide more detail on them.

2.3.1. Ultimate analysis of JS

The elemental analyzer (make: Elementor, model: vario cube) was used to determine the total nitrogen, carbon, and sulfur of the JS and the prepared activated carbon (ACJS). For the CHNS analysis, dried crushed samples were weighed (2–5 mg) in a tin capsule, which is then burned in a reactor at a temperature of 1150°C. The tin capsule with sample melts and the tin promotes a violent reaction (flash combustion) in a momentarily enriched oxygen atmosphere. A steady flow of helium carrier gas conveyed the combustion products CO2, SO2, and NO2 through a glass column containing tungsten trioxide (WO3) oxidation catalyst and copper reducer, both maintained at 850°C. Nitrogen oxide was converted to N2 at this temperature. After that, the helium also transports the N2, CO2, and SO2. A 2 m long packed column is used to separate them, and a thermal conductivity detector set to 300°C is used to measure the results. The elemental contents of CHNS are expressed as a weight percent. By using the difference, the oxygen contents were computed.

2.3.2. Proximate analysis of JS

The process listed below was used to calculate the JS sample's moisture content: Vials that had been previously weighed were filled with 5g of sample. To find the sample's moisture content, the vials were dried in an oven set to 110°C, then moved into a desiccators for a full hour. The vials were then weighed again.

Utilizing the ASTM D2866-94 technique, the ash content was determined. One gram (1.0 g) of dry JS sample was put in a porcelain crucible and cooked to 450°C in a muffle furnace. Once the furnace was running for half an hour, the crucible and its contents were moved to another muffle furnace that had been heated to 775±25°C. Within the second muffle furnace, the crucible was

kept for a full hour. This was followed by removing the crucible and letting it cool. After reweighing the crucible and contents, the weight loss was calculated and recorded as the raw sample's ash content. Equation (1) was then used to compute the percentage of ash content (dry basis).

$$\text{Total ash \%} = [(D1 - B1) \div (C1 - B1) \times 100] \quad (1)$$

Where,

B1 = Weight of crucible (g)

C1 = Weight of crucible with original sample (g)

D1 = Weight of crucible with ashes sample (g)

Using the ASTM 5832 technique, the volatile organic matter content (wt %) was calculated. A crucible with a cover was filled with around 1 g of the known-weight JS sample. For seven minutes, the covered crucible was kept in a muffle furnace set to 4950 °C. After that, the covered crucible was weighed after being allowed to cool to room temperature in desiccators. It was thought that the percentage of weight loss represented the percentage of volatile materials.

$$\text{Volatile organic content \%} = (D1 - B1) \div (C1 - B1) \times 100, \quad (2)$$

Where,

B1 = Weight of crucible (g)

C1 = Weight of crucible with original sample (g)

D1 = Weight of crucible with burnt sample (g)

Fixed carbon is a calculated value and it is the resultant of summation of percentage

Moisture, ash, and volatile matter subtracted from 100.

$$\text{Fixed carbon\%} = [100 - (\text{moisture\%} + \text{ash\%} + \text{volatile matter \%})] \quad (3)$$

2.3.3. Scanning electron microscope (SEM) and EDS analysis

Using scanning electron microscopy (Make: FEI; Model: INSPECT F50) to view the morphology of the samples, the surface characteristics of produced activated carbon (ACJS) and jamun seed powder (JS) were investigated. At 100 mA for emission current and 10 kV for accelerator voltage, the scan parameters were established in stone. The chemical composition of ACJS's surface was also measured at the micro scale using EDS analysis.

2.3.5. Fourier transforms infrared (FTIR) spectroscopy

The presence of functional groups in the prepared samples was investigated by Fourier transform infrared (FTIR) spectroscopy[make: Shimadzu, model: QATR].The occurrence of functional groups in both JS and ACJS were studied in the range of wavelength of 4000cm^{-1} to 400cm^{-1}.

2.4. Batch adsorption studies

An aqueous solution of Ofloxacin (OFC) and Rhodamine B (RhB) in a volume of 200 mL was used as the absorbent in adsorption experiments conducted in batch mode in a round-bottom flask. With the flask remained in an isothermal stirring condition, a mass of the produced ACJS was added. The trials used a known concentration of RhB and OFC and were conducted in a lab incubator shaker with a 180 rpm stirring speed. Within a specific time frame, the same volume of the solution was taken out. By measuring the absorbance of the filtered solution, a UV-visible spectrophotometer (make: Perkin Elmer, Model: lambda 365) was used to examine the extracted sample after it had been filtered via Whatsman filter paper. This allowed for an estimation of the amount of RhB and OFC eliminated. A standard stock solution containing 9.96 ppm of OFC and 15ppm of RhB was made in order to measure the concentrations of the solutions in the UV-visible spectrophotometer. The aqueous stock solution was diluted to prepare the ensuing RhB and OFC solutions. Plotting the standard concentration vs. absorbance graph required measuring the maximum absorbance for OFC at 286 nm and RhB at 554 nm. The mixture solutions of 9.96, 4.98, 2.49, 1.245, 0.6225 ppm OFC and RhB 15, 7.5, 1.875, 0.9375 were created. The relationship between absorbance and concentration that was found based on the figure

$$\text{concentration(OFC)} = \frac{\text{absorbance}}{0.01744} \qquad \text{concentration(RhB)} = \frac{\text{absorbance}}{0.19906}$$

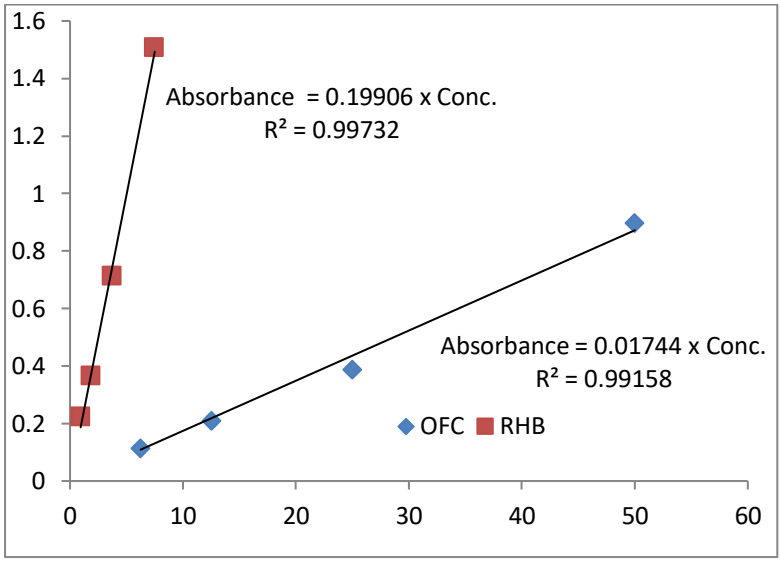


Figure: 5 Standard plots to determine the concentration of OFC & RhB in aqueous solution

The removal percentages of OFC in batch adsorption studies were determined using the following formula

$$\textbf{Removal efficiency}\ (\%) = \frac{C_i - C_f}{C_i} \times 100 \qquad \textbf{(6)}$$

Where, C_i and C_f are the initial and final concentrations of OFC & RhB solution, respectively. The effect of ratio of KOH and CJS was studied to find out the best adsorbent in this study. The effect various parameters such as solution pH, initial concentration, adsorbent dosage, and experimental time on the removal of OFC & RhB were measured. All the experiments were performed in triplicate.

The adsorption capacity (q_e), the amount of adsorbate adsorbed per unit weight of adsorbent at equilibrium, of the prepared ACJS for the removal of OFC, was calculated by the following equation.

$$q_e = \frac{(C_i - C_e)V}{m} \quad (7)$$

where, q_e is the adsorption capacity (mg/g), C_e is the final or equilibrium concentration of OFC & RhB (mg/L), C_i is the initial concentration of OFC & RhB (mg/L), V is the volume of aqueous solution (L), and m is the amount of adsorbent added (g).

2.5 Isotherm models to represent the adsorption process

When a solution comprising of adsorbent, comes in interaction with a solid adsorbent, molecules of adsorbent get transmitted from the solution phase to the compact solid phase until the concentration of adsorbent amongst the solution phase and the compact solid phase are in equilibrium. This is called adsorption equilibrium. Isotherms are the graphs showing distribution process of adsorption between the adsorbed phase and the solution phase at equilibrium. Various isotherm equivalences have been used to describe the equilibrium characteristics of adsorption.

2.5.1. Langmuir isotherm model

The Langmuir isotherm assumes that dynamic equilibrium occurs between adsorbed and free gaseous molecules. The adsorption involves the attachment of only one layer to the surface i.e. only monolayer adsorption is possible onto a surface with a finite number of similar active sites undergoing adsorption. Adsorption occurs at specific homogeneous active sites within the adsorbent. Adsorbent surface is uniform in terms of energy of adsorption. Adsorbed molecules do not interact with each other. Adsorbed molecules do not migrate on the adsorbent surface. The adsorption isotherm derived by Irving Langmuir for the adsorption of a solute from a liquid solution is given by Langmuir[43].

$$q_e = q_m \times \frac{K_L Ce}{1 + K_L.Ce} \quad (8)$$

where, C_e is equilibrium or final concentration (mg/L), q_e is amount of adsorbate adsorbed per unit weight of adsorbent at equilibrium (mg/g), q_m is amount of adsorbate adsorbed per unit weight of adsorbent required for monolayer adsorption i.e. maximum adsorption capacity of the

adsorbent (mg/g) and K_L is amount of adsorbate adsorbed at equilibrium(L/mg). The linear form of Langmuir adsorption isotherm is

$$\frac{C_e}{q_e} = \frac{1}{q_m K_L} + \frac{C_e}{q_m} \quad \textbf{(9)}$$

The plot between C_e and C_e/q_e gives the calculation of Langmuir constants. Langmuir isotherm model can be utilized to evaluate the non-dimensional separation factor or the equilibrium parameter (R_L) by the following equation:

$$R_L = 1/(1 + K_L C_i) \quad \textbf{(10)}$$

Where, is the equilibrium parameter and C_i is the maximum initial concentration. R_L values are indicative of the type of adsorption that is taking place, namely favorable ($0< R_L<1$), unfavorable ($R_L>1$), linear ($R_L =1$) or irreversible ($R_L =0$).

2.5.2. Freundlich isotherm model

An empirical relationship between the solute concentrations in the contact liquid and on the adsorbent surface is known as the Freundlich isotherm. It is obtained by taking into account heterogeneous surfaces that have an uneven heat of adsorption distribution. With an increase in adsorption extent, it is assumed that the heat of adsorption will decrease logarithmically. Additionally, it shows that the in distribution sites' variance with regard to adsorption energy is exponential. It doesn't demonstrate a high enough threshold for monolayer filling. Below is an illustration of the adsorption isotherm's non-linear form as determined by Freundlich [44].

$$q_e = K_F . C_e^{1/n} \quad \textbf{(11)}$$

Where n (dimensionless) is the Freundlich constant, which establishes the attractiveness of the adsorption process, and K_F is the adsorption coefficient, which indicates the quantity of

adsorbate adsorbed on the surface of the adsorbent for a unit equilibrium concentration (L/mg). A quantitative indicator of the adsorption intensity is the value of 1/n, which ranges from 0 to 1. In the neighborhood of 0 for 1/n, there is a noticeable non-uniform distribution. A value greater than one indicates cooperative adsorption, whereas a number less than or equal to one indicates adsorption that takes place in conjunction with a typical Langmuir isotherm. Below is the linear form of the Freundlich adsorption isotherm.

$$\ln q_e = \ln K_F + \frac{1}{n} \ln C_e \qquad (12)$$

The constants K_F and 1/n can be calculated by plotting the graph between $\ln C_e$ and $\ln q_e$.

2.5.3 Temkin adsorption isotherm model

The Temkin isotherm model assumes that adsorption is characterized by a uniform distribution of binding energies, up to a maximum binding energy, and that the adsorption process is affected by indirect adsorbate/adsorbate interactions. It also assumes that the adsorption heat of all molecules decreases linearly with the increase in coverage of the adsorbent surface. Equation (13)[45] can be used to describe the Temkin isotherm.

$$q_e = \frac{RT}{b} \ln K_T + \frac{RT}{b} \ln C_e \qquad (13)$$

Where, K_T is Temkin isotherm constant (L/g) and b is the Temkin constant which is related to binding energy (J/mol). The plot between q_e and $\ln C_e$ gives the calculation of constants of Temkin isotherm.

2.6 Adsorption kinetic studies

The process by which solute molecules adhere to an adsorbent's surface is known as adsorption. Either a batch or column arrangement is used for the adsorption process. The rate at which a solute is retained or released from an aqueous solution to a solid surface at a specific adsorbent dosage, temperature, flow rate, and solution pH is described by the kinetics of adsorption. There

are two primary processes involved in adsorption: chemical adsorption (chemisorptions) and physical adsorption (physisorption). While chemisorptions entail the creation of a strong bond via the transfer of electrons between the solute and the adsorbent, physical adsorption results from weak van der Waals forces of attraction. One of the key concepts that must be comprehended before any adsorbent can be applied is adsorption kinetics. A linear or non-linear kinetics analysis is used in every adsorption process. The kinetics that predicts the adsorbent-adsorbate interaction includes the intra-particle (IP), pseudo-first-order (PFO), and pseudo-second-order (PSO) models. Almost all sorption processes have made extensive use of the first two models. Any model's applicability is contingent upon the degree of error, as measured by the sum of squared errors (SSE) or the correlation coefficient (R^2). The adsorption kinetics under batch adsorption experiments have been studied using the linear forms.

2.6.1 Pseudo first order kinetics

Analyzing adsorption data from the adsorption of adsorbate in aqueous solutions is mostly done using pseudo-first-order kinetics. The rate of adsorption is described by the following process, which is proportional to the number of unoccupied binding sites on adsorbents:

$$\frac{dq_t}{dt} = k_1(q_e - q_t) \qquad (14)$$

Where, q_t is the adsorbent adsorbed onto adsorbent at time t (mg/g), q_e is the equilibrium adsorption capacity (mg/g), and k_1 is the pseudo first order rate constant per min. The integral of Eq. (14) from t=0 to t=t and q_t= 0 and qt=q_t yields a linear expression of pseudo 1st order, Eq. (15).

$$\ln(q_e - q_t) = \ln q_e - k_1 t \qquad (15)$$

The value of k_1 is determined by plotting $\ln(q_e - q_t)$ vs. t.

2.6.2. Pseudo second order kinetics

The adsorption of adsorbate onto adsorbents is described by pseudo 2nd order kinetics, in which the rate of solute adsorption is proportional to the available sites on the adsorbent. The strong chemical bonding between adsorbate and functional groups on the surface of adsorbents is responsible for the adsorption. Here, the amount of solute on the adsorbent surface determines the reaction rate; the driving force,$(q_e - q_t)$, is proportional to the total number of active sites on the adsorbent. The following is the mechanism:

$$\frac{dq_t}{dt} = k_2(q_e - q_t)^2 \qquad (16)$$

Where, k_2 is the pseudo 2nd order rate constant (g/mg·min). The integral of Eq. (16) from t=0 to t=t and q_t=0 and q_t= q_t yields a linear expression of pseudo second order, Eq. (17).

$$\frac{t}{q_t} = \frac{1}{k_2 q_e^2} + \frac{t}{q_e} \qquad (17)$$

A plot of t/q_t against t should demonstrate a linear system, from which the amount of adsorbate adsorbed at equilibrium (q_e, mg/g) and the equilibrium rate constant of pseudo 2nd order sorption (k_2,g/mg·min) can be evaluated from the slope and intercept, respectively. The pseudo 2nd order kinetic model has been applied successfully to determine chemisorptions in several sorption systems.

2.7 Intra-particle diffusion model

To study the rate-limiting step during adsorption, the intra-particle diffusion model has been extensively used. Mass transfer of the adsorbate (film diffusion), surface diffusion, and pore diffusion are all involved in the adsorption of a solute in a solution. However, surface and pore diffusion can happen at the same time. Film diffusion is an independent phase. Weber and Morris [46] investigated intra-particle diffusion, and this model's linearized form is provided as

$$q_t = k_{ip} t^{\frac{1}{2}} + C \qquad (18)$$

Where, k_{ip} is the intra-particle diffusion constant (mg/g.min$^{0.5}$) and *C* is the boundary layer thickness. The values of *C* determines the boundary layer effect higher values, the greater the effect. The plot of q_t vs. $t^{1/2}$ gives a linear function. If the line passes through the origin, intra-particle diffusion controls the adsorption process. However, on many occasions, the plot does not pass through the origin and it gives multiple linear sections; these sections correspond to different mechanisms that control the adsorption process. There are four main mechanisms that describe the transfer of solute from a solution to the adsorbent. The first is called mass transfer (bulk movement) of solute particles as soon as the adsorbent is dropped into the solution. This process is too fast, thus it is not considered during the design of kinetic systems. The second mechanism is called film diffusion; it involves the slow movement of solutes from the boundary layer to the adsorbent's surface. When the solute reaches the surface of the adsorbent, they move to the pores of the adsorbent—third mechanism. The final mechanism involves rapid adsorptive attachment of the solute on the active sites of the pores; being a rapid process, it is not considered during engineering design of kinetics. If the system is characterized by poor mixing, small solute size, and low concentration, film diffusion becomes the rate controlling step; otherwise, intra-particle diffusion controls the process.

2.8 Adsorption thermodynamic studies

Chemical thermodynamics, according to scientist Jacobus Van't Hoff, for a particular chemical reaction calculates the system's internal heat energy, enthalpy, entropy, and free energy values throughout a chemical or physical transformation and examines how these depend on the reaction dynamics. The primary parameters that control the feasibility and spontaneity of chemical reactions are the examination of the thermal parameters that accompany the processes and the thermal properties of the reactants, such as Gibbs free energy change (ΔG^0), change in entropy (ΔS^0), and enthalpy (ΔH^0). This could help to get information about the equilibrium and set forward a general estimate concerning the spontaneity of the response.

The Gibbs free energy change (ΔG^0) is related to the adsorption equilibrium constant by the standard Van't Hoff equation:

$$\Delta G^0 = -RT \ln K \qquad (19)$$

According to thermo chemistry, the Gibbs free energy change (ΔG^0) is also related to the change in entropy (ΔS^0) and heat of adsorption (ΔH^0) at fixed temperature. It is shown by the following equation:

$$\mathbf{\Delta G^0 = \Delta H^0 - T\Delta S^0} \qquad \mathbf{(20)}$$

Combining the above two equations, result in the following equation:

$$\mathbf{\ln K = \frac{-\Delta G^0}{RT} = \frac{\Delta S^0}{R} - \frac{\Delta H^0}{R}\frac{1}{T}} \qquad \mathbf{(21)}$$

Where K_i is the single point or distribution coefficient and is the ratio of q_e *to* C_e. ΔG^0 is the free energy change in kJ/mol, ΔH^0 is the change in enthalpy in kJ/mol, ΔS^0 is the change in entropy in kJ/mol.K, T_i *is* the absolute temperature in K, and R_i is the universal gas constant, i.e., 8.314 J/mol.K. Thus, thermodynamic parameters S^0 and H^0 can be determined by the intercept and slope of the linear Van't Hoff plot, i.e., ln*K* versus *(1/*T), respectively. A batch adsorption study was carried out at various temperatures to determine the thermodynamic parameters.

CHAPTER 3

RESULTS AND DISCUSSION

3.1Characterization

3.1.1 Proximate and elemental analysis

The proximate composition of jamun seed is 28.1 wt% moisture, 18.6 wt% ash, 20.4 wt% volatile matter, and 32.9 wt% fixed carbon, which makes it suitable precursor for obtaining activated carbon. The ultimate analysis performed in CHNS analyzer is shown in Table 3. For JS and ACJS.

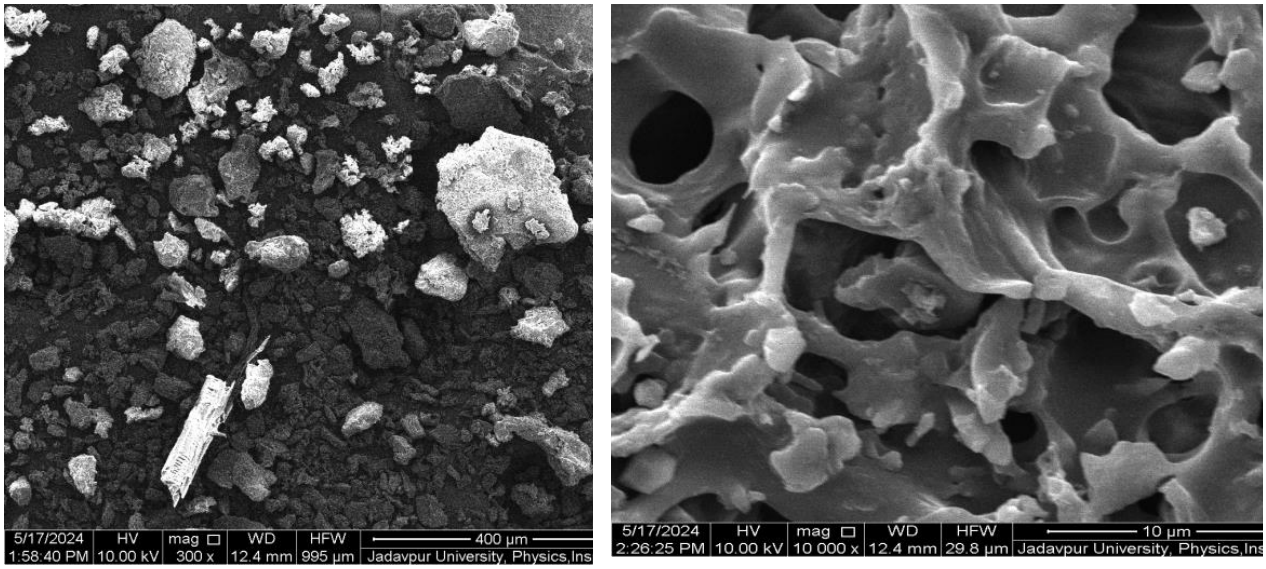
Table.3 the CHNS analysis of JS & ACJS

(%)	C	H	N	S
JS	55.68	15.91	1.85	0
ACJS	61.37	2.480	1.36	0.009

3.1.2. SEM (FESEM) - EDS

One of the most effective and popular surface analytical methods is scanning electron microscopy (SEM), which makes it possible to examine the composition and morphology of a wide range of materials in contemporary science. Figure 6 displays the results of the FESEM analyzer's analysis of the surface micrographs of jamun seed powder (JS) and activated jamun seed powder (ACJS).The figure shows how the surface properties have significantly changed upon activation. In order for the OFC and RhB to interact with the adsorbent, a larger surface area may have been necessary due to the non-uniform surface morphology of the ACJS as an adsorbent, which included many irregular surface features such as pits, channels, ridges, and cracks. Furthermore, adsorption on the surface of ACJS is facilitated by a variety of micro- and macro pores. Furthermore, it was discovered that the varied-sized surface pores were responsible for the effective adsorption performance. The pores had sufficient size to let the molecules of RhB and OFC pass through and adsorb on the surface following their interaction with the functions located there.

Although it can yield semi-quantitative results as well, the energy dispersive spectroscopy (EDS) approach is primarily utilized for qualitative material examination. Figure 7 displays the prepared ACJS EDS spectrum. It was clear from the EDS spectra that the jamun seed included just one C atom, whereas the KOH sample contained only two K and O atoms. The major reaction, which is thought to have occurred between KOH and C, is responsible for this outcome. It is anticipated that a reaction with potassium hydroxide will break down a significant amount of carbon [47]. As a result, the activated carbons produced by KOH activation include more potassium and oxygen. In addition, the EDS spectrum of ACJS displayed that ACJS contains carbon, potassium, and oxygen as its main elements, and KOH reacts with CJS to form the mostly oxidative compound K_2O.



(a) (b)

Figure: 6 SEM morphology of (a) JS and (b) ACJS

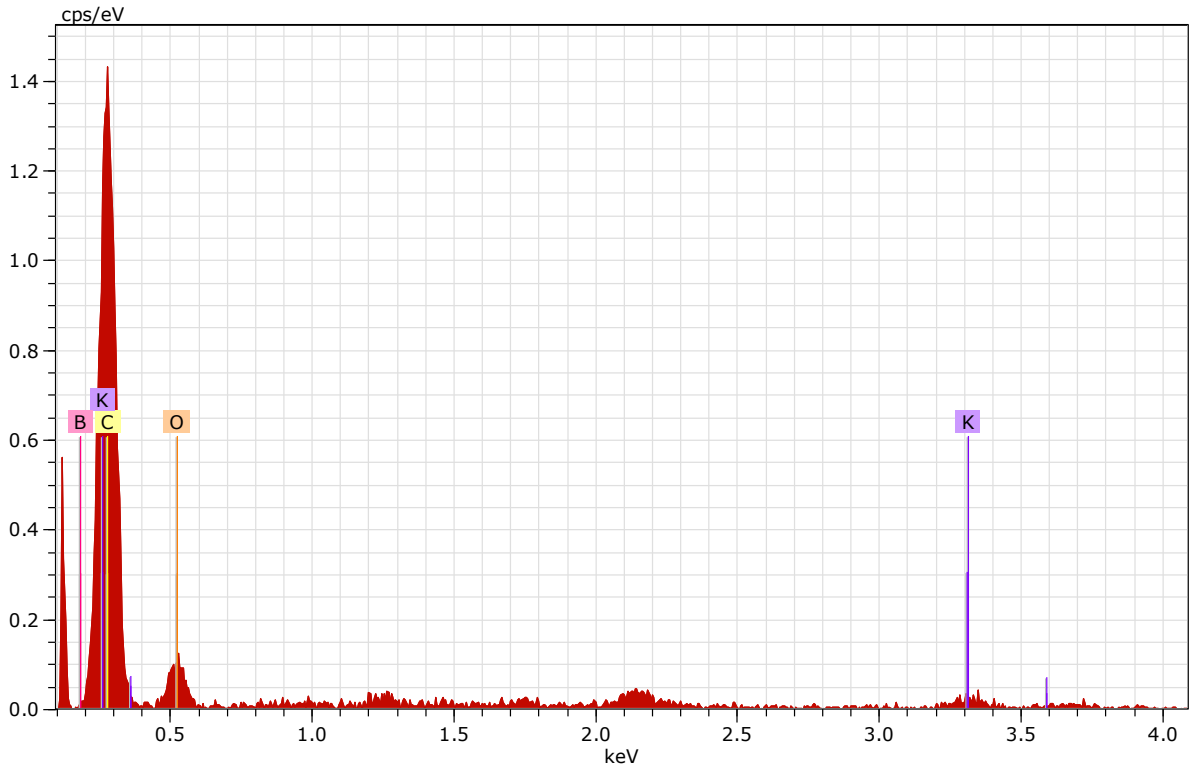
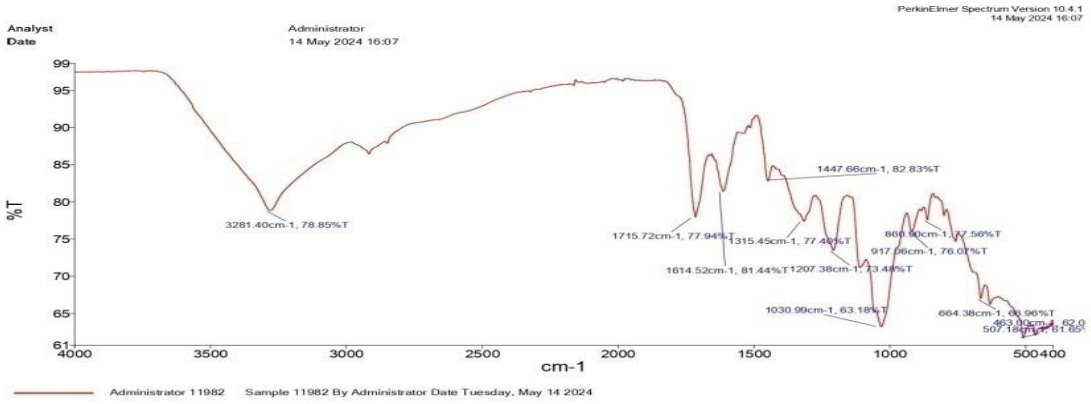


Figure: 7 EDS spectrum of ACJS

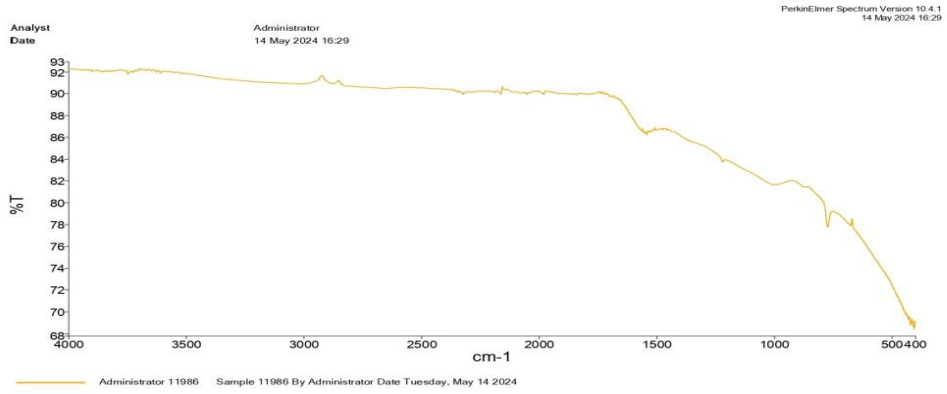
3.1.3. FTIR analysis

FTIR analysis, or Fourier-transform infrared spectroscopy, provides an infrared spectrum of a material's absorption or emission by gathering high-resolution spectral data across a wide spectral range. At each wavelength, it shows how much of a sample is absorbing a single wavelength of infrared light. Figure 8 displays the results for both JS and ACJS. The functional groups were found in the FTIR spectrum between 400–4000 cm^{-1}. O–H stretching (alcohol group) is shown by a wide band in the raw JS at around 3281.40 cm^{-1}. Additionally, cellulosic components are evident in this peak. The asymmetric C–H band alkyl groups (methyl and methylene group) are shown by the band at 1715.72cm^{-1}, which verifies the presence of alkyl groups. Aromatic compounds are represented by the band 1614 cm^{-1} (C=C ring stretching). The peak of 1030.99cm^{-1} validated the C–O stretching components of alcohol and aliphatic ether. As can be seen in the picture, ACJS has a higher absorbance than JS sample because the activated sample has a lower transmittance than the carbonized sample. While aromatic groups are still

discernible, all strong peaks, such as those representing hexagonal, alkyl, and alkane groups, vanished during carbonization and the subsequent KOH activation.



(a)



(b)

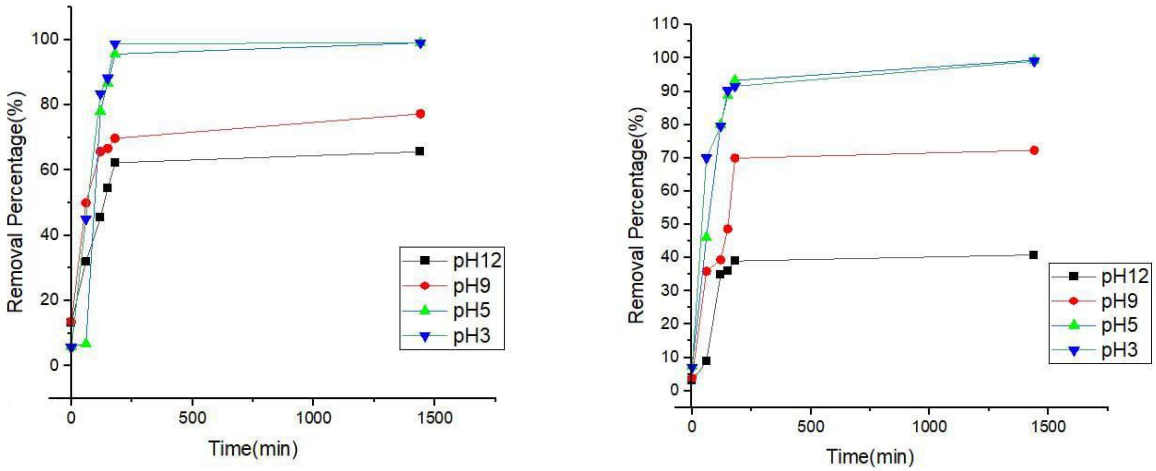
Figure 8: FTIR spectrum of (a) JS and (b) ACJS

3.2. Batch adsorption studies

3.2.1. Effect of solution pH

The effect of pH on the OFC and RhB adsorption onto adsorbent, ACJS, was carried out at room temperature of 303K with the adsorbent dosage of 1g/L, initial concentration of OFC 0.6225ppm and RhB 0.9375ppm , for 180 minute and it is shown in Figure . It can be seen from figure that the adsorption is strongly dependent on pH. OFC and RhB removal increases with an increase in pH initially but, it decreases at higher pH before going through the optimum value. The highest percentage of Ofloxacin adsorption was recorded at pH 5 and highest percentage of RhB adsorption was recorded at pH 3. Ofloxacin slightly acidic in nature and Rhodamine B can exist in equilibrium between two forms; the "open" form dominates in acidic condition while the "closed" form is colorless in basic condition. The Ofloxacin and RhB exist in different species at different ranges of pH [54].The adsorption will be governed by the pH 4 of the solution, it can alter the adsorbent surface charge and chemical properties of the prepared ACJS with OFC and RhB solution [26,29]. As OFC contains negatively charged COO^- ion, at pH 5, slightly acidic medium has the highest removal rate of 98% due to the high ionic interaction between OFC and the charged surface of ACJS and Rhodamine B is an amphoteric dye. It has both positively and negatively charged groups on the molecule, at pH 3 has the highest removal rate of 99%. However, it is usually listed as basic as it has an overall positive charge. . It may be due to the fact that at a low pH value near 4, the H^+ ion concentration in the solution is attached the OH^- ion of OFC in ACJS surface and as a result at pH ~5, the adsorption increases [31, 55]. At highly acidic conditions, at low pH ~3, the removal rate of OFC is 98 % and RhB is 76%. At extremely low and high pH, cationic repulsion occurs and chemical change will also occur between OFC and surface of ACJS, which causes removal rate decreases. And at pH =5, a $\pi - \pi$ interaction occur between –OH group , and aromatic ring of OFC and ACJS, adsorption capacity of ACJS increases[28,56]. And it can be seen that aromatic ring of OFC and π-π interaction should play major role on the removal of OFC from aqueous solution. [57]A possible hydrogen bonding may also occurs between ACJS surface and phenolic – OH groups of OFC and increases adsorption on ACJS surface[56]. Also OFC has fluorine group which has high electron withdrawing ability, and carboxyl group on aromatic ring has high π acceptor ability which also take part on adsorption [58]. But at pH ~9 to pH ~10, at high value of pH, 20% of OFC has zwitterionic form and as a results decreases the adsorption of OFC on ACJS.[54] At very high pH or very low pH

high electrostatic repulsion will occur between OFC and active surface of ACJS.[59] So, pH of the solution for adsorption process was played a major important role for removal of OFC using ACJS from aqueous solution. The effect of solution pH on RhB adsorption was thoroughly studied over a pH range of 3 to 12, with the adsorption rate exhibiting a significant trend in response to pH changes. From pH 3 to pH 5, the removal capacity increased and reached a maximum removal of 99% at pH 5. However, as the pH of the solution increased further, the removal capacity decreased. The outcomes demonstrated that a pH of 5 was ideal for the adsorption studies that followed.



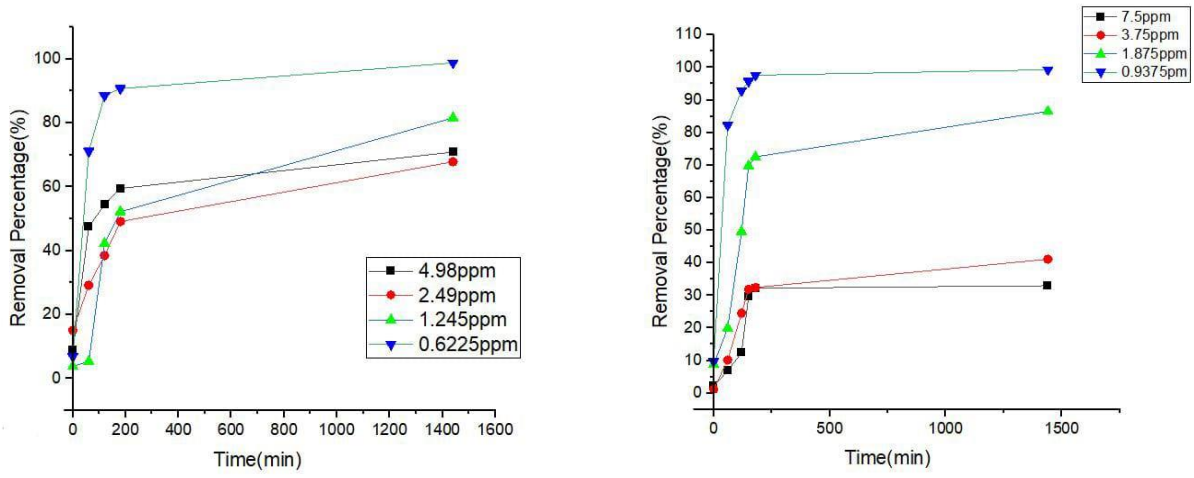
(a) OFC (b) Rhodamine B

Figure: 9 Effect of solution pH on removal of (a) OFC and (b) RhB

3.2.2. Effect of initial concentration OFC and RhB

To study effect of initial concentration of OFC and RhB, prepared aqueous solution of OFC and RhB, at various concentration like, 4.98 & 7.5 ppm, , 2.49 & 3.75 ppm, 1.245 & 1.875 ppm, 0.6225 & 0.9375ppm, with pH=4 ,therefore adsorbent dosage 1g/L ACJS added on it. The incubator shaking speed 180 rpm, mixing time 180 minute. Effect of initial concentration is more important to calculate the capacity of prepared adsorbent, ACJS. Effect of initial concentration on the removal of OFC and RhB is shown in Figure 10. After nearly equilibrium reached, the

percentage of removal for 4.98 & 7.5ppm ppm solution are 54% for OFC and 32 % for RhB, for 2.49 & 3.75 ppm solution the removal percentage 49% for OFC and 32% for RhB, for 1.245 & 1.875 ppm solution the removal percentage is 52% for OFC and 72% for RhB, for 0.6225 & 0.9375 ppm OFC and RhB solution the removal percentage are 90% for OFC and 97% for RhB. With increasing initial concentration of OFC and RhB, the capacity of ACJS increases, but at the same removal efficiency decreases broadly, that was because the adsorbent surface area was fixed and active pore was insufficient for adsorbing large amount of OFC and RhB molecule in aqueous solution. The equilibrium adsorption capacity with the change in initial concentration of OFC and RhB is shown in Figure 10. Here with increasing concentration, no of active sites which act as driving force for adsorption [62] are filled, as a result removal efficiency decreases.



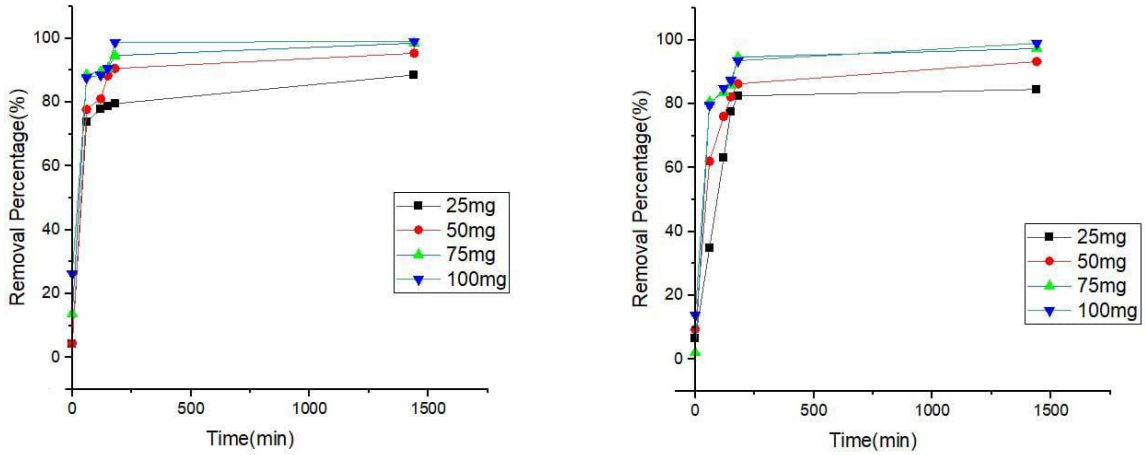
(a) OFC (b) Rhodamine B

Figure: 10 Effect of initial concentration of OFC and RhB on removal efficiency of ACJS

3.2.3. Effect of adsorbent dosage

The effect of ACJS dosages on removal of OFC and RhB at 0.6225 ppm of initial concentration of OFC and 0.9375 ppm of initial concentration of RhB with solution pH of 4 for 180 minutes adsorption time is shown in Figure 11. The amount of dosage was varied from 0.025 to 0.1 g/L of OFC and RhB solution under the optimized condition of agitation time. The result shows that by increasing the amount of adsorbent, the percentage removal also increases. At 0.025g/L ACJS dosage, the removal percentage of OFC & RhB were obtained as 79 % & 82% whereas,

with the adsorbent dosage of 0.1 g/L, the removal percentage of OFC & RhB were found as 98% & 99%. Various factors are reported which can cause the effect of adsorbent dosage. Those includes: (a) with an increase in the adsorbent dosage, the unsaturation of adsorption sites may lead to drop in adsorption capacity (b) agglomeration of adsorbent particles at higher doses may lead to reduce in the surface area and increase the diffutional path length[60,61].



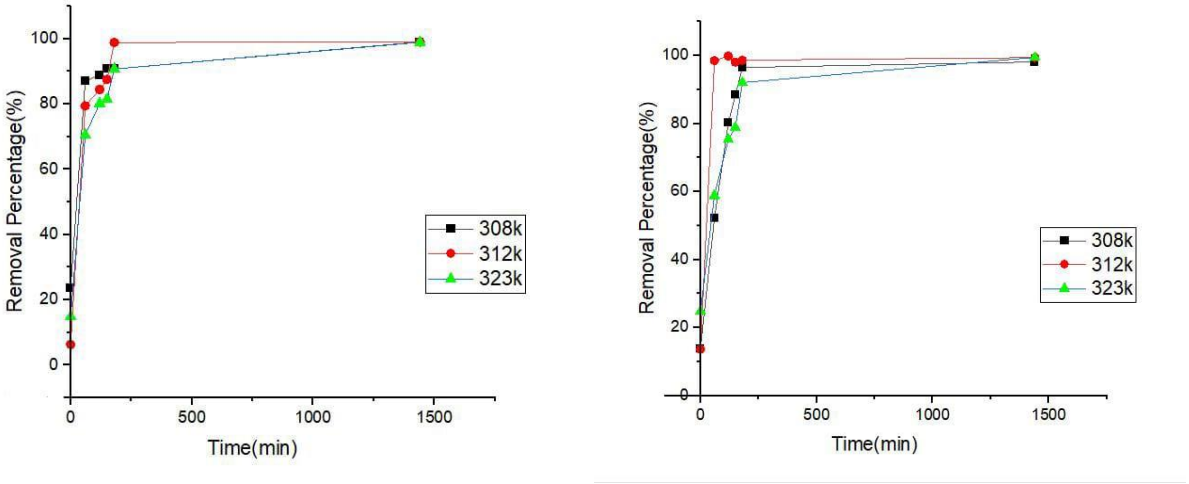
(a) OFC (b) Rhodamine B

Figure: 11 Effect of ACJS dosages on removal of (a) OFC and (b) RhB

3.2.4 Effect of temperature

After analyzing various parameters like pH, adsorbent dosage, mixing time, and initial concentration, the effect of temperature was determined. To determine the impact of temperature on the adsorption of OFC and RhB, we studied 3 different temperatures, from 25^{o}C to 60^{o}C, at pH=4 , adsorbent dosage 0.1g/l, initial concentration of OFC 0.6225ppm and initial concentration of RhB 0.9375ppm, and shaking speed is 180rpm. At 35^{o}C the removal efficiency is 88% of OFC & 97% RhB, and at 60^{o}C the removal efficiency is 71% of OFC & 85%RhB. From the experimental study, we see that as temperature increases from 35^{o}C to 50^{o}C the removal efficiency decreases from 88% to 71% for OFC & 97% TO 85% for RhB, which shows

that the adsorption of OFC and RhB is exothermic in nature. [55]. the removal of OFC and RhB is desirable at low temperatures.



(a) OFC (b) Rhodamine B

Figure 12: Effect of temperature on the removal of OFC and RhB

3.3. Isotherm studies

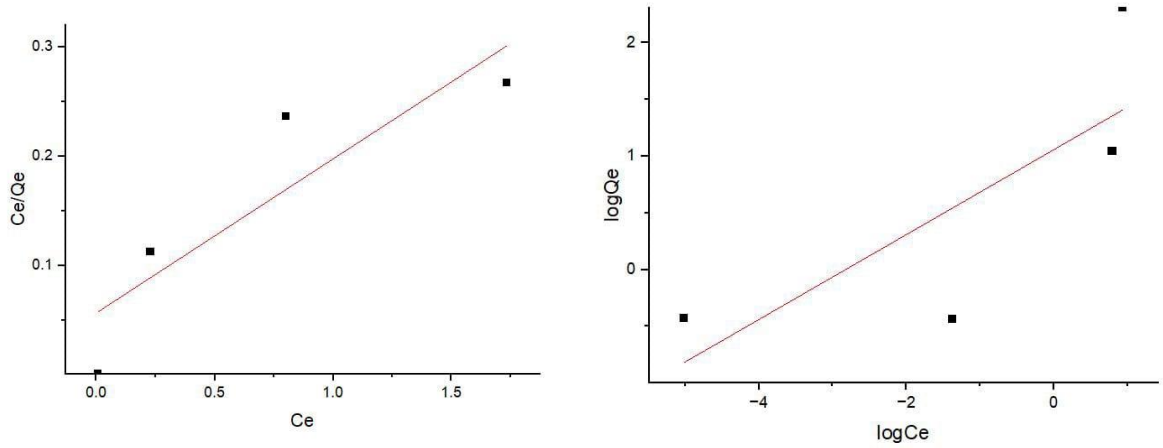
The adsorption isotherm is the most crucial characteristic in the adsorption technique wastewater treatment process since it describes the entire operation. Whether a process is linear or non-linear is predicted by the isotherm model. Examine the isotherm model at specific temperatures, pH levels, and adsorbent dosages by varying the OFC concentration from 0.6225 ppm to 4.98 ppm and the Rhodamine B concentration from 0.9375 ppm to 7.5 ppm. It is necessary to take equilibrium concentration into account when creating an isotherm model. Numerous scientists presented their models in an effort to forecast the adsorption isotherm. Table 4 lists the different adsorption isotherm findings from this experiment.

Table 4. Experimental results on various adsorption isotherms

Adsorption Isotherm	Isotherm type	Equation	Plot	Results of Parameters	
Langmuir Isotherm model	Non linear	$q_e = q_{max} \times \frac{K_L Ce}{1 + K_L . Ce}$	q_e vs. C_e	OFC	RhB
				q_{max}(mg/g)= 11.43 K_L(Lmg^{-1}) =0.235 R^2 = 0.945	q_{max}(mg/g) = 12.14 K_L (Lmg^{-1}) =0.413 R^2 = 0.971
	Linear	$\frac{C_e}{q_e} = \frac{1}{q_{max} K_L} + \frac{C_e}{qmax}$ $R_L = 1/(1 + K_L C_0)$	$\frac{C_e}{q_e}$ vs. C_e	q_{max} (mg/g) = 23.26 R^2 = 0.983 R_L=0.012	q_{max}(mg/g) =22.73 R^2 = 0.976 R_L=0.091
Freundlich Isotherm model	Nonlinear	$q_e = K_F C_e \wedge \frac{1}{n}$	q_e vs C_e	K_F (mg/g)(mg/L)^n=2.43 q_{max} = 22.19 n (g/L)= 0.53 (1/n)=1.89 R^2 =0.961	K_F (mg/g)(mg/L)^n=2.21 q_{max} =23.19 n (g/L)=0.51 (1/n)=1.96 R^2 =0.971
	Linear	$logq_e = logK_F + (1/n)logC_e$	logq_e vs. logC_e	K_F (mg/g)(mg/L)^n=2.51	K_F (mg/g)(mg/L)^n=2.03

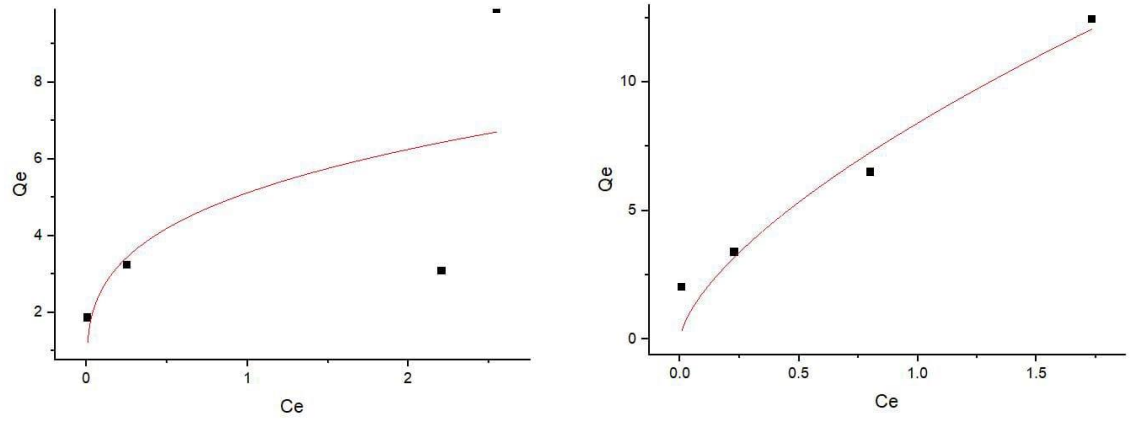
				q_{max} =14.19 n(g/L)= 0.42 (1/n)=2.38 R^2= 0.989	q_{max} =20.35 n(g/L)= 0.58 (1/n)=1.72 R^2= 0.956
Temkin Isotherm model	Linear	$q_e = \frac{RT}{b} lnK_T + \frac{RT}{b} lnC_e$	q_e vs. lnC_e	K_T(Lmg^{-1}) = 6.35 b(j/mol)=0.00 0855 R^2 =0.997	K_T(Lmg^{-1}) = 0.0174 b(j/mol)=2.38 R^2 =0.997

After examining the several adsorption isotherms, the following table shows that q_{max} (mg/g) = 11.43 (OFC) & 12.14 (RhB) are the maximum adsorption capacity and R^2 = 0.945 and 0.971 are the maximum regression coefficient value for the linear isotherm of the Langmuir adsorption model. However, the maximum adsorption capacity for the Langmuir isotherm's nonlinear model are 23.26(mg/g) and 22.73(mg/g). Ultimately, the comparison between the regression coefficient and adsorption capacity with the different models of the Langmuir adsorption isotherm indicates that the linear model's adsorption capacity is higher than the non-linear Therefore, the adsorption is favorable for the linear Langmuir adsorption isotherm, $0< R_L < 1$. [63] The linear and non-linear graphs are given in Figure 13(a) and Figure 13(b), respectively.



OFC **RhB**

Figure: 13 (a) Langmuir linear adsorption isotherm plot.

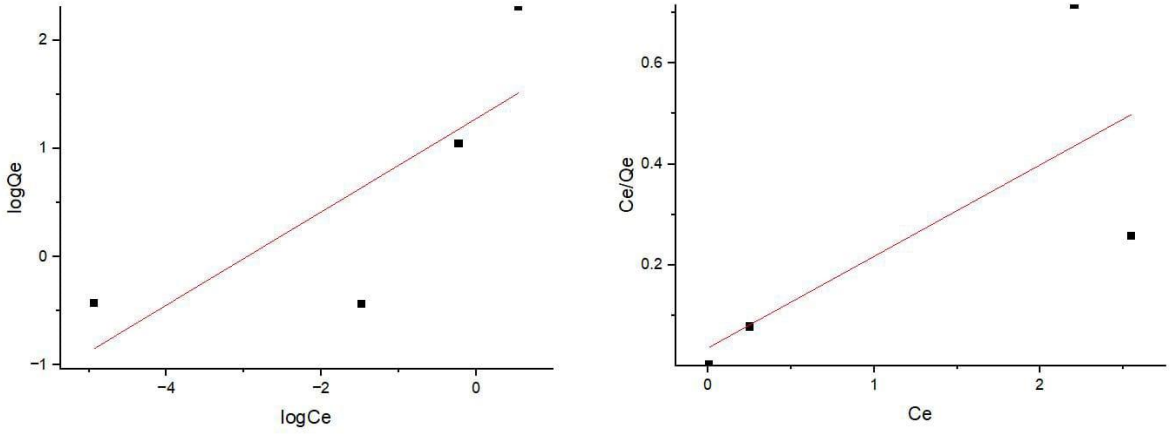


OFC **RhB**

Figure: 13 (b) Langmuir non linear adsorption isotherm plot.

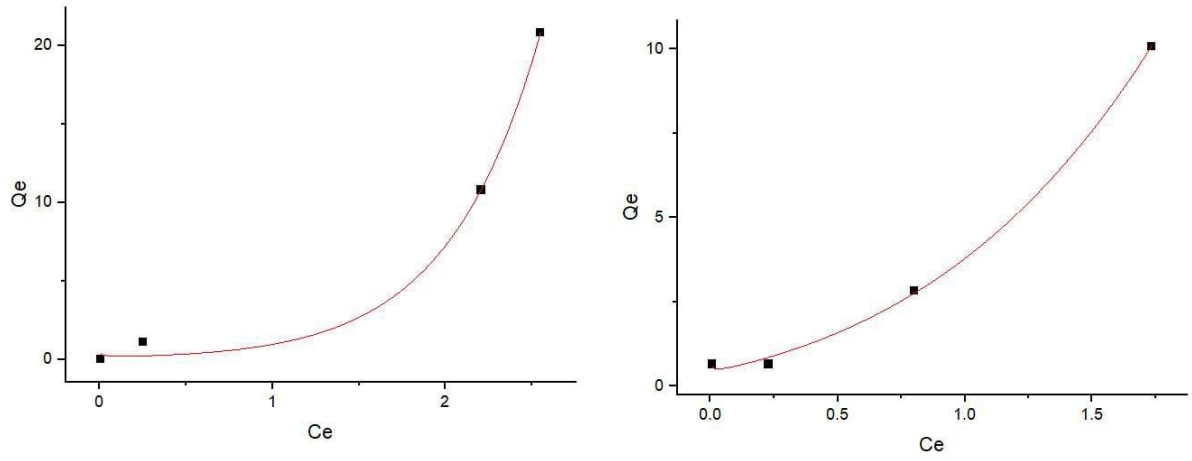
Following the experiment, the regression coefficients for Freundlich the nonlinear model and the linear model were found to be 0.961 and 0.989 for OFC and 0.971 and 0.956 for RhB, respectively. The Freundlich constant are 2.43(OFC) and 2.21(RhB) in non linear and 2.51(OFC) and 2.03(RhB) in linear. The linear isotherm's computed (1/n) value 2.38(OFC) and 1.72(RhB), while the nonlinear isotherm's is 1.89(OFC) and 1.96(RhB). Comparing the linear and nonlinear

Freundlich adsorption isotherms, the linear isotherm's regression coefficient was larger. The adsorption process is favorable, according to the n values. [64]Figure 16(a) and Figure 16(b), respectively displays both the linear and non-linear plots of the Freundlich adsorption isotherm.



OFC RhB

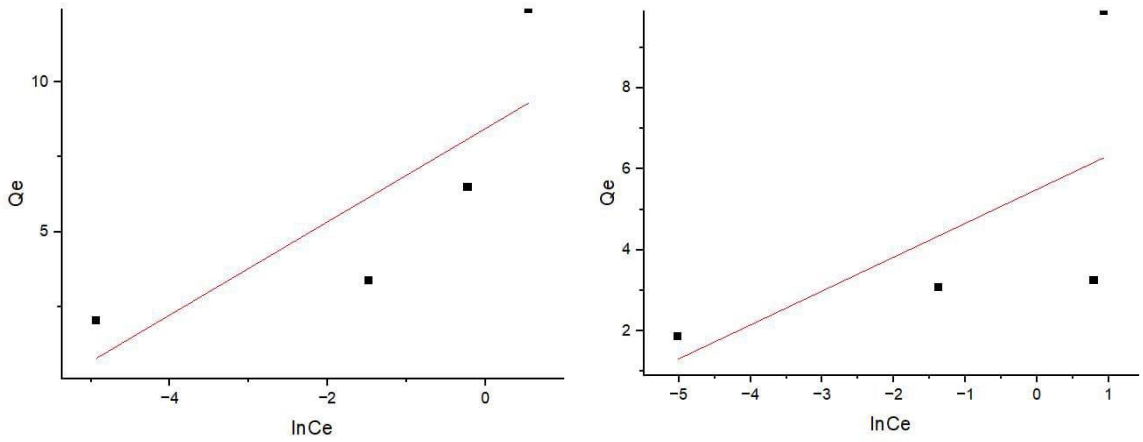
Figure: 14 (a) Linear Freundlich adsorption isotherm model



OFC RhB

Figure: 14 (b) Non linear Freundlich adsorption isotherm model

The heat and binding energy needed for adsorption or heat of adsorption investigations are connected to the Temkin adsorption isotherm. In this example, we plot equilibrium capacity against q_e vs. $\ln C_e$, the logarithm of equilibrium concentration. The Temkin constant, K_T, can be calculated from the intercept. The Temkin adsorption isotherm's regression coefficient value in these investigations are 0.997 (R^2 = 0.997) for OFC and 0.997 (R^2 = 0.997) for RhB, indicating that the adsorption of OFC and RhB are incompatible with the Temkin adsorption isotherm. K_T = 6.35 (l/mg) for OFC and 0.0174(l/mg) for RhB are the Temkin constant. Figure 16 shows the Temkin adsorption isotherm plot. The Langmuir adsorption isotherm > Freundlich adsorption isotherm > Temkin adsorption isotherm was discovered by comparing the regression coefficient values.



OFC **RhB**

Figure 15: Temkin adsorption isotherm

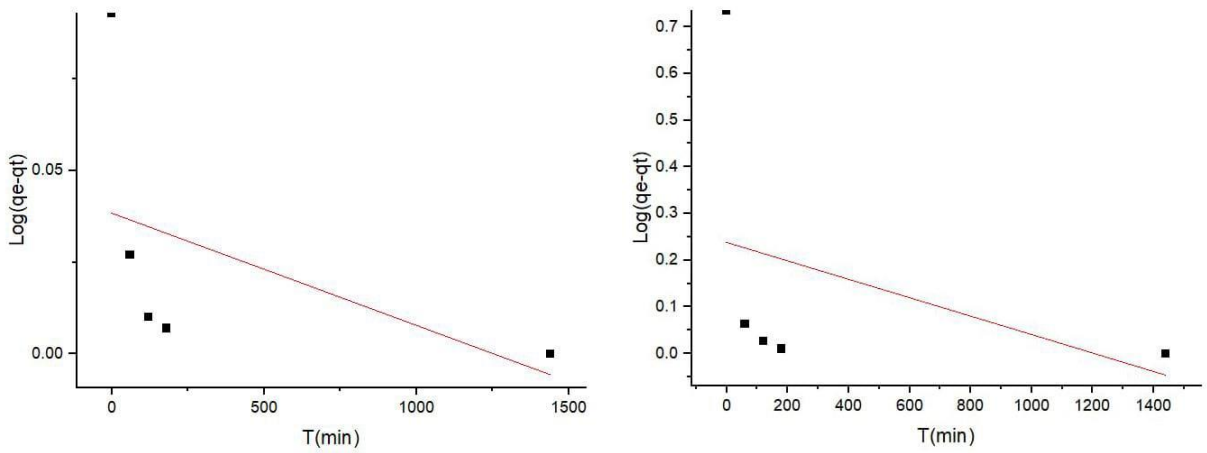
3.4. Kinetic Studies on Adsorption

Table 5. Results on adsorption kinetic model

Kinetic model	**Type**	**Equation**	**Parameter**		**Experimental capacity q_e(mg/g)**
Pseudo 1st order model	Linear	$log(q_e - q_t) = logq_e - \frac{K_1}{2.303}t$	**OFC**	**RhB**	12.44 (OFC)
			q_e = 12.44 (mg/g) R^2=0.981 K_1= 0.0015	q_e = 1.87(mg/g) R^2=0.991 K_1=0.0013	1.87 (RhB)

Pseudo 2nd order model	Linear	$\frac{t}{q_t} = \frac{1}{K_s q^2{}_{eq}} + \frac{1}{q_{eq}}(t)$	K_s=0.00034 R^2 =0.996	K_s=0.041 R^2 =0.981	
Intra-particle diffusion model	Linear	$q_t = K_i t^{(\frac{1}{2})} + C$ q_t vs. $t^{(1/2)}$	R^2 = 0.975 K_i= 0.021 C = 11.193	R^2 =0.971 K_i= 0.0013 C = 0.143	

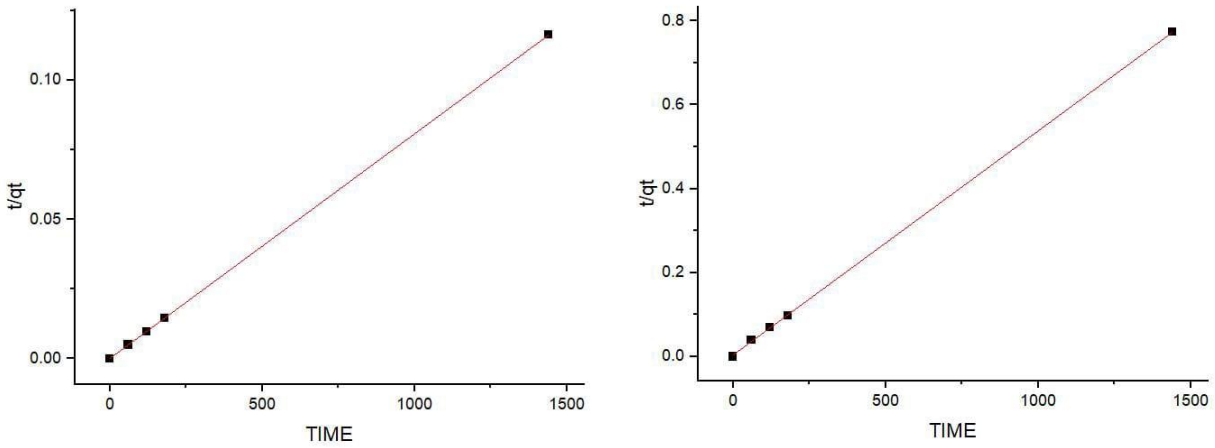
Table 5 provides the data regarding adsorption kinetics. Plotting log (q_e-q_t) vs. t in the pseudo first order model allows us to determine the model's rate constant and adsorption capacity based on the intercept and slope. The estimated equilibrium capacity value qe derived from the linear form of the pseudo-1st order model, is significantly smaller than the experimental capacity value. And the linear 1st model's rate constant, K_1 = 0.0015 for OFC and 0.0013 for RhB. Below is the linear pseudo first order kinetics graph.



OFC **RhB**

Figure: 16 (a) the plot of linear pseudo 1st order kinetics

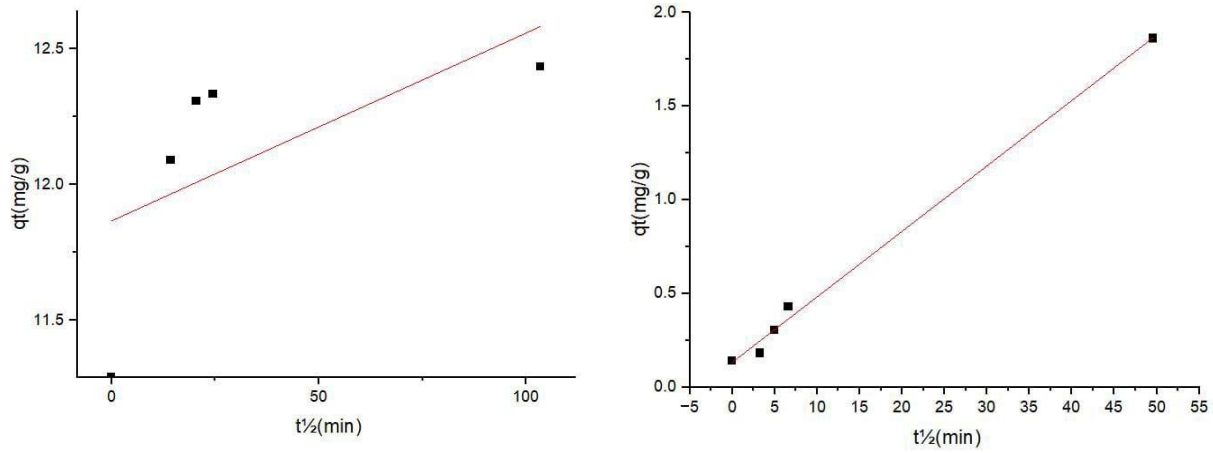
We used the pseudo 2nd order model to fit the data after evaluating the pseudo 1st order model. Plotting t/q_t vs. t for the pseudo 2nd order linear model allows us to determine the value of the 2nd order rate constant and the capacity value (adsorbed OFC concentration and RhB concentration) based on the slope and intercept. The adsorption capacity, q_e = 12.43559 (mg/g) of OFC and 1.87(mg/g) for RhB, for the linear pseudo-2nd order equation and the regression coefficient, R^2 = 0.996 and 0.981, were observed in Table 5. Additionally, 0.00034 and 0.041 were discovered to be the second-order rate constant in K_s linear kinetics.



OFC **RhB**

Figure: 16 (b) the plot of linear pseudo 2nd order kinetics.

Plotting q_t vs. $t^{(1/2)}$ in the intra particle diffusion model provides the value of the K_i intra particle diffusion constant, while the intercept provides the C value. The values of the diffusion model include the intra particle diffusion rate constant, k_i = 0.021 for OFC and K_i = 0.0013 for RhB; regression coefficient; boundary layer-related model constant, C = 11.193 for OFC and C= 0.143 for RhB, and standard deviation. In this case, the C value indicates the expected thickness of the boundary layer. Since the C value is larger, the analysis demonstrates that OFC adsorption affects the boundary layer [65]. The Adsorption Model will follow the Intra particle Diffusion Model if the straight line in the plot of q_t versus $t^{(1/2)}$ passes through the origin; however, in this instance, the straight line does not pass through the origin, hence the Adsorption does not follow the Intra particle diffusion model, but from the C value and regression coefficient R^2 value, the adsorption is influenced by the Intra particle diffusion model.



OFC **RhB**

Figure: 17 The plot of q_t vs. $t^{(1/2)}$ for intra particle diffusion model

3.5. Thermodynamics study on adsorption

In order to verify that the adsorption process is feasible and spontaneous, thermodynamic parameters are crucial. They offer the data required to plan an adsorption procedure. Typically, thermodynamic parameters consist of entropy (ΔS), Gibbs free energy (ΔG), and heat of enthalpy (ΔH). It is crucial to explain the viability of OFC and RhB adsorption by using the ACJS thermodynamic parameter computation. The thermodynamic parameters computed value. Table 7 displays the values of enthalpy, entropy, and Gibbs free energy. Figure 18 plots $\ln K_d$ vs. (1/T) using Van't Hoff equation. We determine the entropy, ΔS^o, and the enthalpy, ΔH^o, of this batch adsorption of OFC and RhB from the slope and intercept of the plot, $\ln K_d$ vs. (1/T). The equation $\Delta G^o = \Delta H^o – T\Delta S^o$ is used to compute the Gibbs free energy ΔG^o at various temperatures, including 308K, 323K and 333K The results are discuss below.

As can be observed in Table 6 below, during the adsorption of OFC and RhB, the entropy ΔS_o negative, which measures the degree of disorder between adsorbate and adsorbent molecules, decreases.[55]. The literature revealed that the entropy in the adsorption of OFC and RhB were likewise negative, indicating a decrease in the unpredictability of the adsorption process. [28–55]. Reduces in the entropy of this batch adsorption process occur when OFC and RhB adheres

to the surface of ACJS due to the force of attraction between the molecules of ACJS with OFC and RhB [34].

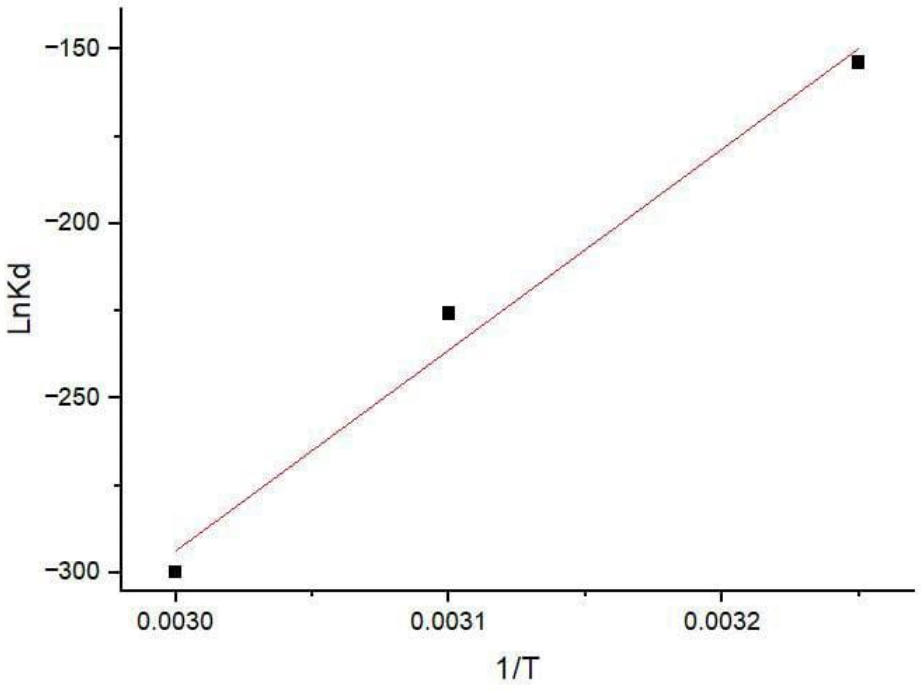


Figure 18: Thermodynamic study on adsorption

At 308 K, the Gibb's free energy (G) are -3.23 KJ/mol for OFC and -3.92 KJ/mol for RhB; at 323 K, it is -5.40KJ/mol for OFC and -6.10 KJ/mol for RhB; at 333 K, it is -6.81KJ/mol for OFC and 7.50KJ/mol for RhB. A negative ΔG value indicates that the adsorption of OFC and RhB are feasible and spontaneous at temperatures ranging from 308K to 333K. Also the adsorption is exothermic in nature. It implies that the adsorption of RhB and OFC increases with temperature. Plotting ln (1-Θ) vs. (1/T) yielded the activation energy (E_a) that is displayed in Figure 19. This graph is based on Arrhenius equation, which describes the temperature, depends of reaction rate. From the equation ln (1- Θ) = $-E_a/RT$+ Constant, where Θ represents the surface coverage, which is the fraction of adsorption sites on the surface that are occupied by adsorbents, from adsorption isotherm Θ = (Q/Q_m). From this equation we get Ea = -R × (slope), where R is gas constant (8.314/mol.K).

Ea = -8.314 J/mol·K × (-1578.94737)

= 13151.11 J/mol

= 13.15 kJ/mol.

The activation energy value was found to be as 13.15 kJ/mol.

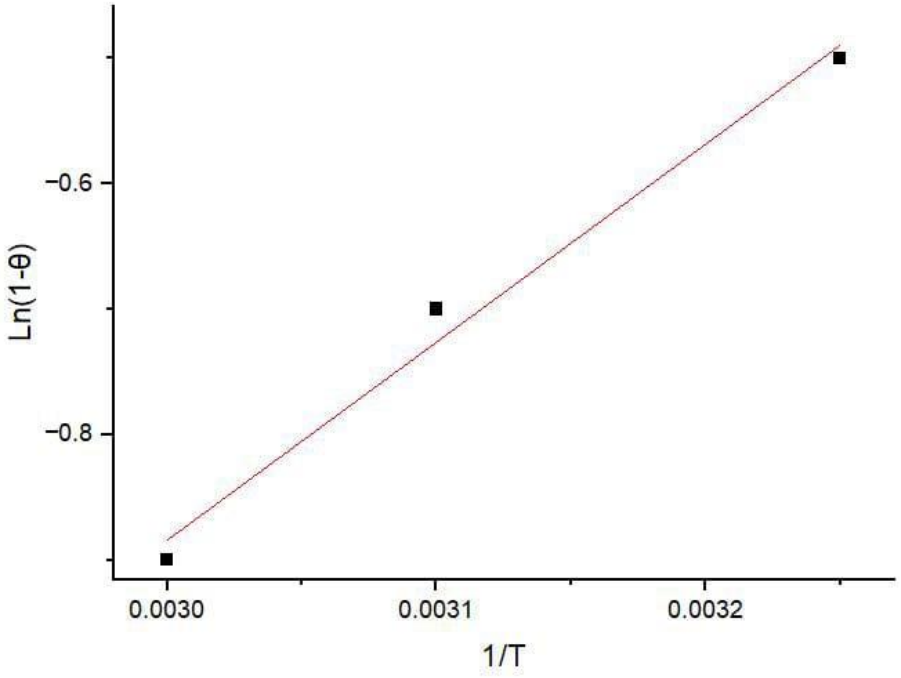


Figure: 19 Determination of activation energy on adsorption.

Table.6 Thermodynamics studies of (A) OFC & (B) RhB

(A) Adsorption Thermodynamics Data of OFC

Temperature (k)	**C_e (ppm)**	**Q_e(mg/g)**	**ln K_c**	**ΔS (J/mol.K)**	**ΔH (K./mol)**
308	**0.005739756**	**174.12**	**5.164**	**139.31**	**39.63**
323	**0.0058647**	**170.51170562859**	**5.143**		
333	**0.006342574**	**157.66469575285**	**5.067**		

(B) Adsorption Thermodynamics study of Rhodamine B

Temperature (K)	C_e (ppm)	Q_e (mg/g)	$\ln K_c$	ΔS (J/mol.K)	ΔH (K./mol)
308	0.017655135	56.640745029703	4.043	141.41	39.63
323	0.005737619	174.28832412887	5.165		
333	0.005099425	196.10054074724	5.283		

CHAPTER 4

4. Conclusion

The adsorbent (activated carbon) used in this project is made from jamun seeds and is used to remove the color dye Rhodamine B and the medicinal medication Ofloxacin. The most effective ratio for removing OFC was 1:1 between KOH and Pyrolyzed jamun seed powder. When KOH was used to activate the powdered jamun seed, 366.39 m2/g of activated carbon was produced. 180 minutes of batch adsorption research produced the greatest removal percentage of 97% of OFC and 98% of RhB by ACJS. The pseudo-2nd order linear model of adsorption kinetics was in agreement with the linear Langmuir model, which provided the best fit for the adsorption isotherm. Based on the study of thermodynamics, ΔS = 139.31 J/mol.K, ΔH =39.63 KJ/mol for OFC and ΔS = 141.41 J/mol.K, ΔH =39.63 KJ/mol for RhB. The ACJS's highest capacity to remove Rhodamine B and OFC was found to be 40.39 mg/g. Therefore, it can be said that the activated carbon made from bio waste (jamun seed) was highly effective in removing Rhodamine B and Ofloxacin from an aqueous solution. Without sacrificing the effectiveness of removing OFC and RhB from aqueous solution, the activated carbon made from powdered jamun seeds is very reasonably priced and can be used up to several times to remove pollutants.

References

[1] J. Akhtar, N.A.S. Amin, K. Shahzad, A review on removal of pharmaceuticals from water by adsorption, Desalin. Water Treat. 57 (2016) 12842–12860. https://doi.org/10.1080/19443994.2015.1051121.

[2] A.J. Watkinson, E.J. Murby, D.W. Kolpin, S.D. Costanzo, The occurrence of antibiotics in an urban watershed: From wastewater to drinking water, Sci. Total Environ. 407 (2009) 2711–2723. https://doi.org/10.1016/j.scitotenv.2008.11.059.

[3] P. Paíga, M. Correia, M.J. Fernandes, A. Silva, M. Carvalho, J. Vieira, S. Jorge, J.G. Silva, C. Freire, C. Delerue-Matos, Assessment of 83 pharmaceuticals in WWTP influent and effluent samples by UHPLC-MS/MS: Hourly variation, Sci. Total Environ. 648 (2019) 582–600. https://doi.org/10.1016/j.scitotenv.2018.08.129.

[4] C.G. Daughton, T.A. Ternes, Pharmaceuticals and personal care products in the environment: Agents of subtle change?, Environ. Health Perspect. 107 (1999) 907–938. https://doi.org/10.1289/ehp.99107s6907.

[5] M.D. Hernando, M. Mezcua, A.R. Fernández-Alba, D. Barceló, Environmental risk assessment of pharmaceutical residues in wastewater effluents, surface waters and sediments, Talanta. 69 (2006) 334–342. https://doi.org/10.1016/j.talanta.2005.09.037.

[6] J.L. Martínez, Effect of antibiotics on bacterial populations : a multi-hierachical selection process [version 1 ; referees : 2 approved] Referee Status :, 6 (2017) 1–10. https://doi.org/10.12688/f1000research.9685.1.

[7] D.I. Andersson, D. Hughes, Antibiotic resistance and its cost: Is it possible to reverse resistance?, Nat. Rev. Microbiol. 8 (2010) 260–271. https://doi.org/10.1038/nrmicro2319.

[8] D.I. Andersson, The biological cost of mutational antibiotic resistance : any practical conclusions ?, (n.d.). https://doi.org/10.1016/j.mib.2006.07.002.

[9] S. Monarca, D. Feretti, C. Collivignarelli, L. Guzzella, I. Zerbini, G. Bertanza, R. Pedrazzani, The influence of different disinfectants on mutagenicity and toxicity of urban wastewater, Water Res. 34 (2000) 4261–4269. https://doi.org/10.1016/S0043-1354(00)00192-5.

[10] A. Gonsioroski, V.E. Mourikes, J.A. Flaws, Endocrine disruptors in water and their effects on the reproductive system, Int. J. Mol. Sci. 21 (2020). https://doi.org/10.3390/ijms21061929.

[11] Z. He, S. Zang, Y. Liu, Y. He, H. Lei, A multi-walled carbon nanotubes-poly(l-lysine) modified enantioselective immunosensor for ofloxacin by using multi-enzyme-labeled gold nanoflower as signal enhancer, Biosens. Bioelectron. 73 (2015) 85–92. https://doi.org/10.1016/j.bios.2015.05.054.

[12] E. Hapeshi, A. Achilleos, A. Papaioannou, L. Valanidou, N.P. Xekoukoulotakis, D. Mantzavinos, D. Fatta-Kassinos, Sonochemical degradation of ofloxacin in aqueous solutions, Water Sci. Technol. 61 (2010) 3141–3146. https://doi.org/10.2166/wst.2010.921.

[13] J. Michael, Formulary Forum, Ann. Pharmacother. 23 (1989) 839–846.

[14] K. Kümmerer, Antibiotics in the aquatic environment - A review - Part I, Chemosphere. 75 (2009) 417–434. https://doi.org/10.1016/j.chemosphere.2008.11.086.

[15] Y. Deng, A. Debognies, Q. Zhang, Z. Zhang, Z. Zhou, J. Zhang, L. Sun, T. Lu, H. Qian, Effects of ofloxacin on the structure and function of freshwater microbial communities, Aquat. Toxicol. 244 (2022) 106084. https://doi.org/10.1016/j.aquatox.2022.106084.

[16] P. Kovalakova, L. Cizmas, T.J. McDonald, B. Marsalek, M. Feng, V.K. Sharma, Occurrence and toxicity of antibiotics in the aquatic environment: A review, Chemosphere. 251 (2020) 126351. https://doi.org/10.1016/j.chemosphere.2020.126351.

[17] M.S. de Ilurdoz, J.J. Sadhwani, J.V. Reboso, Antibiotic removal processes from water & wastewater for the protection of the aquatic environment - a review, J. Water Process Eng. 45 (2022) 102474. https://doi.org/10.1016/j.jwpe.2021.102474.

[18] A. Al-ahmad, V. Mersch-sundermann, Biodegradability of some antibiotics , elimination of the genotoxicity and a ection of wastewater bacteria in a simple test, 40 (2000).

[19] M.A. Al-Omar, Chapter 6 Ofloxacin, 2008. https://doi.org/10.1016/S1871-5125(09)34006-6.

[20] A.Y.C. Lin, T.H. Yu, C.F. Lin, Pharmaceutical contamination in residential, industrial, and agricultural waste streams: Risk to aqueous environments in Taiwan, Chemosphere. 74 (2008) 131–141. https://doi.org/10.1016/j.chemosphere.2008.08.027.

[21] D.G.J. Larsson, C. de Pedro, N. Paxeus, Effluent from drug manufactures contains extremely high levels of pharmaceuticals, J. Hazard. Mater. 148 (2007) 751–755. https://doi.org/10.1016/j.jhazmat.2007.07.008.

[22] S. Castiglioni, R. Bagnati, R. Fanelli, F. Pomati, D. Calamari, E. Zuccato, Removal of pharmaceuticals in sewage treatment plants in Italy, Environ. Sci. Technol. 40 (2006) 357–363. https://doi.org/10.1021/es050991m.

[23] J. Liu, X. Wu, J. Liu, C. Zhang, Q. Hu, X. Hou, Ofloxacin degradation by Fe3O4-CeO2/AC Fenton-like system: Optimization, kinetics, and degradation pathways, Mol. Catal. 465 (2019) 61–67. https://doi.org/10.1016/j.mcat.2018.12.020.

[24] M.O. Composite, Fenton Degradation of Ofloxacin Using a, (2020) 2–11. https://doi.org/10.3390/ECCS2020-07528.

[25] A. Thakur, N. Sharma, A. Mann, Materials Today : Proceedings Removal of ofloxacin hydrochloride and paracetamol from aqueous solutions : Binary mixtures and competitive adsorption, Mater. Today Proc. 28 (2020) 1514–1519. https://doi.org/10.1016/j.matpr.2020.04.833.

[26] V. Bhatia, A.K. Ray, A. Dhir, Enhanced photocatalytic degradation of ofloxacin by co-doped titanium dioxide under solar irradiation, Sep. Purif. Technol. 161 (2016) 1–7. https://doi.org/10.1016/j.seppur.2016.01.028.

[27] P.C. Papaphilippou, O.M. Marinica, E. Tanas, F. Mpekris, T. Stylianopoulos, V. Socoliuc, T. Krasia-christoforou, Ofloxacin Removal from Aqueous Media by Means of Magnetoactive Electrospun Fibrous Adsorbents, (2022).

[28] Q. Kong, X. He, L. Shu, M. sheng Miao, Ofloxacin adsorption by activated carbon derived from luffa sponge: Kinetic, isotherm, and thermodynamic analyses, Process Saf. Environ. Prot. 112 (2017) 254–264. https://doi.org/10.1016/j.psep.2017.05.011.

[29] R.A. Wuana, R. Sha'Ato, S. Iorhen, Aqueous phase removal of ofloxacin using adsorbents from Moringa oleifera pod husks, Adv. Environ. Res. 4 (2015) 49–68. https://doi.org/10.12989/aer.2015.4.1.049.

[30] G. Kaur, N. Singh, A. Rajor, Ofloxacin adsorptive interaction with rice husk ash: Parametric and exhausted adsorbent disposability study, J. Contam. Hydrol. 236 (2021) 103737. https://doi.org/10.1016/j.jconhyd.2020.103737.

[31] M. Ashraf, M.M. Galal, M.E. Matta, Removal of danofloxacin and ofloxacin as different generations of fluoroquinolones from aqueous solutions through the adsorption process using granular activated carbon: A comparative study, mechanism elucidation, and applicability investigation, Alexandria Eng. J. 71 (2023) 679–690.

https://doi.org/10.1016/j.aej.2023.03.096.

[32] P. King, N. Rakesh, S.B. Lahari, Y.P. Kumar, V.S.R.K. Prasad, Biosorption of zinc onto Syzygium cumini L.: Equilibrium and kinetic studies, Chem. Eng. J. 144 (2008) 181–187. https://doi.org/10.1016/j.cej.2008.01.019.

[33] M. Vinayagam, R. Suresh Babu, A. Sivasamy, A.L. Ferreira de Barros, Biomass-derived porous activated carbon from Syzygium cumini fruit shells and Chrysopogon zizanioides roots for high-energy density symmetric supercapacitors, Biomass and Bioenergy. 143 (2020) 105838. https://doi.org/10.1016/j.biombioe.2020.105838.

[34] R. Araga, S. Soni, C.S. Sharma, Fluoride adsorption from aqueous solution using activated carbon obtained from KOH-treated jamun (Syzygium cumini) seed, J. Environ. Chem. Eng. 5 (2017) 5608–5616. https://doi.org/10.1016/j.jece.2017.10.023.

[35] Removal of heavy metal from waste water bt adsorption using chem-bio modifued bio degradable waste with the help of silver nano particles from syzygium cumini seeds extracts, (2018) 1298–1318. 1. Vani Shanmuganathan 2. Manivannan-R , Department of Chemistry GCW Kumbakonam.

[36] A. Banerjee, N. Dasgupta, B. De, In vitro study of antioxidant activity of Syzygium cumini fruit, Food Chem. 90 (2005) 727–733. https://doi.org/10.1016/j.foodchem.2004.04.033.

[37] F.I. Chavan, M. Husain, S.S. Paul, I. Mohammad, Domestic Wastewater Treatment Using Jamun Leaves As Adsorbents, Int. J. Innov. Eng. Sci. 6 (2021) 1. https://doi.org/10.46335/ijies.2021.6.10.1.

[38] C. Jampani, A. Naik, K.S.M.S. Raghavarao, Purification of anthocyanins from jamun (Syzygium cumini L.) employing adsorption, Sep. Purif. Technol. 125 (2014) 170–178. https://doi.org/10.1016/j.seppur.2014.01.047.

[39] E.S. Rigobello, A.D.B. Dantas, L. Di Bernardo, E.M. Vieira, Removal of diclofenac by conventional drinking water treatment processes and granular activated carbon filtration, Chemosphere. 92 (2013) 184–191. https://doi.org/10.1016/j.chemosphere.2013.03.010.

[40] E. Arany, J. Láng, D. Somogyvári, O. Láng, T. Alapi, I. Ilisz, K. Gajda-Schrantz, A. Dombi, L. Kohidai, K. Hernádi, Vacuum ultraviolet photolysis of diclofenac and the effects of its treated aqueous solutions on the proliferation and migratory responses of Tetrahymena pyriformis, Sci. Total Environ. 468–469 (2014) 996–1006.

https://doi.org/10.1016/j.scitotenv.2013.09.019.

[41] M. Negarestani, M. Motamedi, A. Kashtiaray, A. Khadir, M. Sillanpää, Simultaneous removal of acetaminophen and ibuprofen from underground water by an electrocoagulation unit: Operational parameters and kinetics, Groundw. Sustain. Dev. 11 (2020). https://doi.org/10.1016/j.gsd.2020.100474.

[42] B. Maryam, V. Buscio, S.U. Odabasi, H. Buyukgungor, A study on behavior, interaction and rejection of Paracetamol, Diclofenac and Ibuprofen (PhACs) from wastewater by nanofiltration membranes, Environ. Technol. Innov. 18 (2020) 100641. https://doi.org/10.1016/j.eti.2020.100641.

[43] V. Fierro, V. Torné-Fernández, A. Celzard, Highly microporous carbons prepared by activation of kraft lignin with KOH, Stud. Surf. Sci. Catal. 160 (2007) 607–614. https://doi.org/10.1016/s0167-2991(07)80078-4.

[44] A.H. Basta, V. Fierro, H. El-Saied, A. Celzard, 2-Steps KOH activation of rice straw: An efficient method for preparing high-performance activated carbons, Bioresour. Technol. 100 (2009) 3941–3947. https://doi.org/10.1016/j.biortech.2009.02.028.

[45] A. Raza, M. Usman Ali, T. Nisar, S. Ahmad Qasrani, R. Hussain, M. Nawaz Sharif, Proximate Composition of Jamun (Syzygium cumini) Fruit and Seed, J. Agric. Environ. Sci. 15 (2015) 1221–1223. https://doi.org/10.5829/idosi.aejaes.2015.15.7.12700.

[46] T. Unugul, F.U. Nigiz, Preparation and Characterization an Active Carbon Adsorbent from Waste Mandarin Peel and Determination of Adsorption Behavior on Removal of Synthetic Dye Solutions, Water. Air. Soil Pollut. 231 (2020). https://doi.org/10.1007/s11270-020-04903-5.

[47] N. Priyantha, L. Lim, M.K. Dahri, L.B.L. Lim, Dragon Fruit Skin as a Potential Low-Cost Biosorbent for the Removal of Manganese(II) Ions, J. Appl. Sci. Environ. Sanit. 8 (2013) 179–188.

[48] B. Kakavandi, R.R. Kalantary, M. Farzadkia, A.H. Mahvi, A. Esrafili, A. Azari, A.R. Yari, A.B. Javid, Enhanced chromium (VI) removal using activated carbon modified by zero valent iron and silver bimetallic nanoparticles, J. Environ. Heal. Sci. Eng. 12 (2014). https://doi.org/10.1186/s40201-014-0115-5.

[49] O. LAÇİN, F. Demir, B. BASTABAN, Aktif Karbon Üzerine Perteknetat Oksoanyonunun Denge İzoterm Modelinin Belirlenmesi, Sinop Üniversitesi Fen Bilim. Derg. 4 (2019) 37–

46. https://doi.org/10.33484/sinopfbd.486647.

[50] D. A.O, Langmuir, Freundlich, Temkin and Dubinin–Radushkevich Isotherms Studies of Equilibrium Sorption of Zn 2+ Unto Phosphoric Acid Modified Rice Husk, IOSR J. Appl. Chem. 3 (2012) 38–45. https://doi.org/10.9790/5736-0313845.

[51] N. Ayawei, A.N. Ebelegi, D. Wankasi, Modelling and Interpretation of Adsorption Isotherms, J. Chem. 2017 (2017). https://doi.org/10.1155/2017/3039817.

[52] E.D. Revellame, D.L. Fortela, W. Sharp, R. Hernandez, M.E. Zappi, Adsorption kinetic modeling using pseudo-first order and pseudo-second order rate laws: A review, Clean. Eng. Technol. 1 (2020) 100032. https://doi.org/10.1016/j.clet.2020.100032.

[53] A. Aurich, J. Hofmann, R. Oltrogge, M. Wecks, R. Gläser, L. Blömer, S. Mauersberger, R.A. Müller, D. Sicker, A. Giannis, Improved Isolation of Microbiologically Produced (2R,3S)-Isocitric Acid by Adsorption on Activated Carbon and Recovery with Methanol, Org. Process Res. Dev. 21 (2017) 866–870. https://doi.org/10.1021/acs.oprd.7b00090.

[54] M. Özacar, I.A. Şengil, Adsorption of metal complex dyes from aqueous solutions by pine sawdust, Bioresour. Technol. 96 (2005) 791–795. https://doi.org/10.1016/j.biortech.2004.07.011.

[55] H. Joga Rao, P. King, Y. Prasanna Kumar, Application of response surface methodology for optimization of cadmium adsorption in an aqueous solution by activated carbon prepared from Bauhinia Purpurea leaves, Rasayan J. Chem. 11 (2018) 1577–1586. https://doi.org/10.31788/RJC.2018.1144024.

[56] J. Fan, J. Zhang, C. Zhang, L. Ren, Q. Shi, Adsorption of 2,4,6-trichlorophenol from aqueous solution onto activated carbon derived from loosestrife, Desalination. 267 (2011) 139–146. https://doi.org/10.1016/j.desal.2010.09.016.

[57] F. Batool, J. Akbar, S. Iqbal, S. Noreen, S.N.A. Bukhari, Study of Isothermal, Kinetic, and Thermodynamic Parameters for Adsorption of Cadmium: An Overview of Linear and Nonlinear Approach and Error Analysis, Bioinorg. Chem. Appl. 2018 (2018). https://doi.org/10.1155/2018/3463724.

[58] Vibrational Spectra and Analysis of Trans – decahydronaphthalene, 1 (2010) 211–216.

[59] F.R.-R. Matthias Thommes*, Katsumi Kaneko, Alexander V. Neimark, James P. Olivier, J.R. and K.S.W. Sing, Brunauer-Emmett-Teller (BET) surface area analysis, Pure Appl. Chem. 87 (2013) 1051–1069.

https://www.ru.ac.za/media/rhodesuniversity/content/nanotechnology/documents/BET Refilwe Matshitse.pdf.

[60] K. Kinashi, Y. Kambe, M. Misaki, Y. Koshiba, K. Ishida, Y. Ueda, Synthesis, characterization, photo-induced alignment, and surface orientation of poly(9,9-dioctylfluorene-alt-azobenzene)s, J. Polym. Sci. Part A Polym. Chem. 50 (2012) 5107–5114. https://doi.org/10.1002/pola.26338.

[61] L. Xu, J. Zhang, J. Ding, T. Liu, G. Shi, X. Li, W. Dang, Y. Cheng, R. Guo, Pore structure and fractal characteristics of different shale lithofacies in the dalong formation in the western area of the lower yangtze platform, Minerals. 10 (2020). https://doi.org/10.3390/min10010072.

[62] S. Sadaf, H.N. Bhatti, Evaluation of peanut husk as a novel, low cost biosorbent for the removal of Indosol Orange RSN dye from aqueous solutions: Batch and fixed bed studies, Clean Technol. Environ. Policy. 16 (2014) 527–544. https://doi.org/10.1007/s10098-013-0653-z.

[63] M. Crespo-Alonso, V.M. Nurchi, R. Biesuz, G. Alberti, N. Spano, M.I. Pilo, G. Sanna, Biomass against emerging pollution in wastewater: Ability of cork for the removal of ofloxacin from aqueous solutions at different pH, J. Environ. Chem. Eng. 1 (2013) 1199–1204. https://doi.org/10.1016/j.jece.2013.09.010.

[64] S.A. Hassan, F.J. Ali, Assessement of the Ofloxacin (Novecin) Adsorption from aqueous solutions by Two Agricultural Wastes, Int. J. Adv. Sci. Tech. Res. 2 (2014) 950–965.

[65] D. Lin, B. Xing, Adsorption of phenolic compounds by carbon nanotubes: Role of aromaticity and substitution of hydroxyl groups, Environ. Sci. Technol. 42 (2008) 7254–7259. https://doi.org/10.1021/es801297u.

[66] B. Peng, L. Chen, C. Que, K. Yang, F. Deng, X. Deng, G. Shi, G. Xu, M. Wu, Adsorption of Antibiotics on Graphene and Biochar in Aqueous Solutions Induced by π-π Interactions, Sci. Rep. 6 (2016) 1–10. https://doi.org/10.1038/srep31920.

[67] H. Peng, B. Pan, M. Wu, Y. Liu, D. Zhang, B. Xing, Adsorption of ofloxacin and norfloxacin on carbon nanotubes: Hydrophobicity- and structure-controlled process, J. Hazard. Mater. 233–234 (2012) 89–96. https://doi.org/10.1016/j.jhazmat.2012.06.058.

[68] H. Liu, W. Liu, J. Zhang, C. Zhang, L. Ren, Y. Li, Removal of cephalexin from aqueous solutions by original and Cu(II)/Fe(III) impregnated activated carbons developed from

lotus stalks Kinetics and equilibrium studies, J. Hazard. Mater. 185 (2011) 1528–1535. https://doi.org/10.1016/j.jhazmat.2010.10.081.

[69] A.A.M. Daifullah, S.M. Yakout, S.A. Elreefy, Adsorption of fluoride in aqueous solutions using KMnO4-modified activated carbon derived from steam pyrolysis of rice straw, J. Hazard. Mater. 147 (2007) 633–643. https://doi.org/10.1016/j.jhazmat.2007.01.062.

[70] A. Chandrasekaran, C. Patra, S. Narayanasamy, S. Subbiah, Adsorptive removal of Ciprofloxacin and Amoxicillin from single and binary aqueous systems using acid-activated carbon from Prosopis juliflora, Environ. Res. 188 (2020) 109825. https://doi.org/10.1016/j.envres.2020.109825.

[71] R. Huang, B. Yang, Q. Liu, K. Ding, Removal of fluoride ions from aqueous solutions using protonated cross-linked chitosan particles, J. Fluor. Chem. 141 (2012) 29–34. https://doi.org/10.1016/j.jfluchem.2012.05.022.

[72] P. Tirkey, T. Bhattacharya, S. Chakraborty, Optimization of fluoride removal from aqueous solution using Jamun (Syzygium cumini) leaf ash, Process Saf. Environ. Prot. 115 (2018) 125–138. https://doi.org/10.1016/j.psep.2017.